

# Venturi Aeration of Bioreactors

Fadzai Kadzinga

Thesis submitted in fulfilment of the academic requirements for the degree of Master of Science in Engineering in the Department of Chemical Engineering

University of Cape Town

February 2015



The copyright of this thesis vests in the author. No quotation from it or information derived from it is to be published without full acknowledgement of the source. The thesis is to be used for private study or non-commercial research purposes only.

Published by the University of Cape Town (UCT) in terms of the non-exclusive license granted to UCT by the author.

## Abstract

Low solubility of oxygen has resulted in high bioreactor energy requirements in order to supply sufficient oxygen to aerobic bioprocesses. It is desirable to reduce energy consumption in bioreactors to benefit environmental sustainability as well as economic feasibility. This is particularly important with the resurgence of interest in bio-based commodity products.

Some research has suggested that venturi aeration of bioreactors will reduce energy consumption by eliminating the need for air compression, while at the same time maintaining or improving oxygen transfer rates. On the other hand, there are findings that suggest venturi aeration has lower energy efficiency than conventional sparging and oxygen transfer rates achieved are too low sustain aerobic biological processes.

A comparison of the aeration of geometrically-similar reactors using the same analytical methods to determine  $k_{La}$  is not available in the literature. This comparison should also address analysis of energy input including energy used for compressing gas sparged into a stirred tank reactor; the investigation of mass transfer rates at higher flow rates (vvm) in venturi-aerated reactors and resulting cell response to these higher flow rates. This is the topic of the dissertation presented.

In this laboratory scale study, venturi aerators were characterised and energy consumption as a function of oxygen mass transfer rates compared with a geometrically identical aerated stirred tank reactor by evaluating the volumetric mass transfer coefficients ( $k_{La}$ ). The  $k_{La}$  was investigated in varying reactor setups using the dynamic gassing-in method.

The mass transfer coefficient in a venturi-aerated reactor was found to depend on liquid flow rate through the venturi aerator and bulk liquid movement in the tank. Liquid flow rates investigated were between 1.3 vvm and 2.6 vvm. The  $k_{La}$  increased with liquid flow rate and was affected by the change in bulk mixing in the tank that resulted from changing the venturi outlet height in the tank. At higher liquid flow rates,  $k_{La}$  as much as doubled by changing the venturi outlet height. Liquid mass balance models suggest that a considerable portion of the oxygen mass transfer occurred in the tank.

Comparison of total power input to the reactor showed that venturi aeration achieved mass transfer rates as high as those in an aerated stirred tank for the same power input. For total power up to 6  $\text{kWm}^{-3}$ , the  $k_{La}$  in the venturi system was similar to that in the stirred tank at an equivalent power input; while the stirred tank gave better mass transfer at higher power input.

The growth of brewer's yeast in the venturi aerated reactor was the same as that in the aerated stirred tank with maximum growth rates of 0.115  $\text{h}^{-1}$  and 0.138  $\text{h}^{-1}$  respectively.

Venturi aeration did not show significantly better energy efficiency than sparged stirred tanks, but can be made more competitive by reducing energy lost when circulating the liquid and optimising fluid hydrodynamics in the tank.

## **Acknowledgements**

To Prof Sue Harrison for her supervision and guidance.

To Dr Tobi Louw for helping me make sense of it.

To all of CeBER for the help, support and input.

To my friends and family for their support.

To the Department of Chemical Engineering for financial assistance.

## Table of Contents

1	Introduction .....	1-1
2	Literature review .....	2-1
2.1	Oxygen mass transfer in bioreactors .....	2-1
2.2	Determination of the mass transfer coefficient ( $k_{La}$ ) in a stirred tank .....	2-3
2.2.1	Sulphite oxidation method .....	2-4
2.2.2	Dynamic gassing in method .....	2-4
2.2.3	Hydrogen peroxide method.....	2-6
2.2.4	Oxygen balance method.....	2-7
2.2.5	Dynamic pressure method.....	2-7
2.3	Factors affecting oxygen transfer and $k_{La}$ in stirred tank reactors .....	2-8
2.3.1	Agitation .....	2-8
2.3.2	Gas flow rate .....	2-9
2.3.3	Broth composition.....	2-9
2.4	Correlation of $k_{La}$ in stirred tank reactors .....	2-10
2.5	Principles of Venturi aeration .....	2-13
2.5.1	Liquid flow rate.....	2-15
2.5.2	Venturi geometry .....	2-15
2.5.3	Venturi-reactor configuration .....	2-16
2.6	Application of venturi aeration to bioreactors .....	2-17
2.7	Cell damage in venturi aerators .....	2-19
2.8	Measuring $k_{La}$ in venturi aerated reactors.....	2-19
2.9	Energy consumption in bioreactors.....	2-21
3	Hypothesis and key questions .....	3-1
3.1	Hypothesis.....	3-2
3.2	Key questions.....	3-2
4	Materials and Methods .....	4-1
4.1	Experimental set-up .....	4-1
4.1.1	Stirred tank reactor.....	4-1
4.1.2	Venturi system .....	4-2

4.1.3	Oxygen measurement equipment.....	4-4
4.2	Dynamic method for measurement of oxygen transfer.....	4-5
4.2.1	Dynamic method in the stirred tank reactor.....	4-5
4.2.2	Dynamic method in the venturi-aerated reactor.....	4-5
4.2.3	Analytical method for $k_La$ determination in the stirred tank.....	4-5
4.2.4	Accounting for lag in electrode response.....	4-7
4.2.5	Analysis of venturi aerated reactor .....	4-8
4.3	Mixing studies in venturi aerated reactor.....	4-11
4.4	Calculation of power.....	4-11
4.5	Aerobic cultivation of Baker's yeast.....	4-12
4.5.1	Microorganism and culture maintenance .....	4-13
4.5.2	Operating conditions.....	4-13
4.5.3	Cell growth analysis.....	4-13
4.5.4	Glucose analysis .....	4-14
4.6	Research approach .....	4-15
5	Results and discussion.....	5-1
5.1	Oxygen Mass Transfer in the Stirred Tank System .....	5-1
5.1.1	OTR and $k_{La}$ as a function of agitation rate and gas flow rate.....	5-1
5.2	Oxygen mass transfer in the venturi system .....	5-4
5.2.1	Mixing in the tank.....	5-7
5.2.2	OTR and $k_{La}$ as a function of liquid flow rate and depth of inlet (tank hydrodynamics) 5-8	
5.2.3	OTR and $k_{La}$ as a function of venturi configuration .....	5-11
5.2.4	Modelling oxygen mass transfer using the Venturi system .....	5-12
5.2.5	Comparison of power input between stirred tank and venturi aerated tank.....	5-14
5.3	Yeast growth and survival in the Venturi aerated system.....	5-15
6	Conclusions and Recommendations.....	6-1
6.1	Conclusions.....	6-1
6.2	Recommendations.....	6-2
7	Bibliography.....	7-1

## Table of Figures

Figure 2.1: Schematic of two-film theory by Whitman .....	2-2
Figure 2.2: Variation of $k_La$ with agitation power for different studies.....	2-11
Figure 2.3: Schematic of a venturi device.....	2-14
Figure 2.4: Setup of a venturi aerator in a semi-batch process .....	2-18
Figure 4.1: Schematic of reactor used in stirred tank experiments .....	4-1
Figure 4.2: Schematic of experimental set-up for venturi aeration experiments (a) shows arrangement of apparatus and (b) shows top-down view of components in the tank .....	4-3
Figure 4.3: Results obtained in the determination of $\tau_r$ .....	4-5
Figure 4.4: Change of DO concentration in the tank with time at agitation power of $5.36 \text{ kW m}^{-3}$ and aeration rate of $12 \text{ L min}^{-1}$ .....	4-6
Figure 4.5: Change of DO concentration in the tank with time at agitation power of $0.509 \text{ kW m}^{-3}$ and $25 \text{ L min}^{-1}$ .....	4-6
Figure 4.6: The difference between $k_La$ calculated with electrode response accounted for ( $k_La$ lag) and $k_La$ measured (no correction) in the stirred tank .....	4-7
Figure 4.7: Change of DO concentration in the tank with time at liquid flow rate of $42 \text{ L min}^{-1}$ and outlet height of 8 cm .....	4-8
Figure 4.8: Change of DO in the tank with time for a venturi aerated reactor at liquid flow rate of $22.2 \text{ L min}^{-1}$ and 4 cm outlet height. ....	4-10
Figure 4.9: Change of conductivity with time after injecting salt for two repeats at a liquid circulation rate of $22.2 \text{ L min}^{-1}$ at an outlet height of 4 cm.....	4-11
Figure 5.1: Variation of $k_La$ with agitation rate at different air flow rates.....	5-2
Figure 5.2: Correlation of $k_La$ with aeration rate and agitation power input .....	5-3
Figure 5.3: Variation of $k_La$ in a stirred tank with total power input .....	5-3
Figure 5.4: Prediction of the variation of pressure drop in the throat of the venturi aerator and air flow rate into the venturi with liquid flow rate through the venturi .....	5-5
Figure 5.5: DO concentration in liquid stream immediately out of the venturi aerator compared to DO concentration in the tank corrected for electrode response time at liquid flow rate of $36.6 \text{ L/min}$ and 4 cm outlet height.....	5-6
Figure 5.6: Change in DO concentration in the tank with time when the air hole is closed compared to when the air hole is open. Liquid flow rate through the venturi aerator was $42 \text{ L min}^{-1}$ at a venturi outlet height of 8 cm .....	5-7
Figure 5.7: Mixing times in venturi aerated tank for a single venturi (Setup 1) at different venturi outlet heights as a function of liquid flow rate.....	5-7
Figure 5.8: Effect of water flow rate and venturi outlet height on $k_La$ .....	5-99

Figure 5.9: Comparison of gas holdup at (a) 22.2 L/min and (b) 36.6L/min for a venturi outlet height of 12 cm .....	5-1010
Figure 5.10: Comparison of $k_{La}$ between a single venturi at venturi outlet heights of 4 cm, 8 cm and 12 cm, and two venturis connected in parallel at an outlet height of 8 cm .....	5-122
Figure 5.11: Difference between measured DO concentration and that predicted by assuming no mass transfer happens in the tank. ....	5-133
Figure 5.12: Effect of liquid flow rate and outlet height on $k_{LaV}$ at different venturi outlet heights and $k_{LaT}$ at different venturi outlet heights .....	5-133
Figure 5.13: Variation of $k_{La}$ with total power input for all conditions in the stirred tank reactor, Single venturi and two venturis in parallel .....	5-155
Figure 5.14: Comparison of growth of <i>S. cerevisiae</i> in the venturi aerated reactor to that in the stirred tank, and glucose consumption in the venturi aerated reactor and in the stirred tank. ....	5-166
Figure 5.15: Growth of <i>S. cerevisiae</i> shake flask inoculated with cells from the aerated stirred tank and cells that had been in the venturi aerated reactor for 15 minutes and 90 minutes compared to growth of <i>S.cerevisiae</i> in the aerated stirred tank .....	5-166



## List of Tables

Table 2.1: Reactor specifications for $k_La$ studies shown in Figure 2.2 .....	2-12
Table 2.2: Typical values for constants in Equation (2.23) for an air- water system in a stirred tank reactor .....	2-13
Table 2.3: Comparison of oxygen transfer in venturi-aerated reactors to sparged reactors.....	2-18
Table 2.4: $k_La$ values for venturi-aerated systems under various operating conditions .....	2-21
Table 4.1: Dimensions of reactor used in stirred tank experiments.....	4-2
Table 4.2: Agitation rates and corresponding power consumption.....	4-2
Table 4.3: Research approach .....	4-15
Table 5.1: Coefficients for the correlation $kLa = C(P/V)^\alpha u^\beta$ .....	5-2
Table 5.2: Rate of air suction into the venturi for varying water flow rates. The air suction rate was not affected by the venturi outlet height. ....	5-9
Table 5.3: Results for the cultivation of yeast in different reactor setups.....	5-17

## Nomenclature

Symbol	Definition	Units
$A_T$	Total interfacial surface area	$\text{m}^2$
$a$	Interfacial surface area per unit reactor volume	$\text{m}^2\text{m}^{-3}$
$C$	Discharge coefficient of venturi air hole	
$C^*$	Saturation concentration of oxygen in the liquid phase corresponding to the bulk gas phase	$\text{mol m}^{-3}$
$C_0$	Initial concentration of oxygen in the liquid phase	$\text{mol m}^{-3}$
$C_A$	Concentration of oxygen in the bulk liquid phase	$\text{mol m}^{-3}$
$C_{Ai}$	Concentration of oxygen at the gas- liquid interface	$\text{mol m}^{-3}$
$C_G^e$	Concentration of oxygen in the exit gas	$\text{mol m}^{-3}$
$C_G^f$	Concentration of oxygen in the inlet gas	$\text{mol m}^{-3}$
$C_{H_2O_2}^f$	feed concentration of $\text{H}_2\text{O}_2$	$\text{mol m}^{-3}$
$C_L$	Concentration of oxygen in the bulk liquid phase	$\text{mol m}^{-3}$
$C_m$	Dissolved oxygen concentration displayed on the DO meter	$\text{mol m}^{-3}$
$C_V$	Concentration of oxygen in the liquid at the venturi outlet	$\text{mol m}^{-3}$
$D$	Impeller diameter	$\text{m}$
$D_{AB}$	Diffusivity of oxygen in water	$\text{m}^2 \text{s}^{-1}$
$D_b$	Bubble diameter	$\text{m}$
$\varepsilon_G$	Gas holdup	
$E$	Specific power input	$\text{Wm}^{-3}$
$F$	Liquid volumetric flow rate	$\text{m}^3\text{s}^{-1}$
$g$	Acceleration due to gravity	$\text{ms}^{-2}$
$g_c$	Dimensional constant	$\text{Pa}$
$\gamma$	Ratio of specific heat for gas=1.395 for air with adiabatic compression	
$H$	Height of liquid in the reactor	$\text{m}$
$H_A$	Henry's law coefficient	$\text{kPa m}^{-3} \text{mol}^{-1}$
$J_A$	Molar flux of oxygen from the gas phase to the liquid phase	$\text{mol m}^{-2} \text{s}^{-1}$
$K$	$(\gamma-1)/\gamma = 0.283$ for air	
$k_L a$	Volumetric mass transfer coefficient	$\text{s}^{-1}$
$k_L a_T$	Volumetric mass transfer coefficient in the tank	$\text{s}^{-1}$
$k_L A_V$	Mass transfer coefficient in the venturi aerator	$\text{m}^3\text{s}^{-1}$
$\mu$	Specific growth rate	$\text{h}^{-1}$

$n$	Impeller agitation rate	rpm
$N_A$	Rate of oxygen transfer from gas phase to liquid phase	$\text{mol s}^{-1}$
$N_{PG}$	Gassed power number	
$OTR$	Rate of oxygen transfer from gas phase to liquid phase	$\text{mol m}^{-3} \text{s}^{-1}$
$OUR$	Oxygen uptake rate	$\text{mol m}^{-3} \text{s}^{-1}$
$P$	Power input	kW
$\pi$	Pressure	Pa or kPa
$\pi_1$	Initial pressure	Pa or kPa
$\pi_2$	Final pressure	Pa or kPa
$p_A$	Partial pressure of oxygen in the bulk gas phase	kPa
$p_{Ai}$	Partial pressure of oxygen at the gas-liquid interface	kPa
$Q_G$	Volumetric gas flow rate	$\text{m}^3 \text{s}^{-1}$
$Q_L$	Volumetric liquid flow rate	$\text{m}^3 \text{s}^{-1}$
$R$	Gas constant	$\text{J mol}^{-1} \text{K}^{-1}$
$\rho$	Density of fluid	$\text{kg m}^{-3}$
$T$	Tank diameter	m
$T_1$	Gas temperature	K
$TDH$	Total dynamic head	m
$\tau_r$	Response time of DO electrode	s
$u_G$	Gas velocity	$\text{ms}^{-1}$
$u_L$	Liquid velocity	$\text{ms}^{-1}$
$V$	Reactor volume	$\text{m}^3$
$w$	Gas mass flow rate	$\text{kg s}^{-1}$
$W$	Specific weight of water	$\text{N m}^{-3}$
$z$	Distance over which diffusion occurs	m

# 1 Introduction

Recently, it has become increasingly important for industrial processes to be environmentally sustainable. There is a push towards bio-based, environmentally responsible products which has led to a resurgence of interest in large scale commodity bioprocesses in which both operating costs are key and environmental impact of the large scale process significant (Yang, 2007).

In a bioreactor, energy is used for temperature control, agitation, and for compressing and pumping gases into the reactor. Thus optimisation of these processes can be targeted to improve energy efficiency of bioreactors. Most aerobic bioprocesses are limited by the availability of oxygen in the reactor, therefore it is crucial to ensure sufficient oxygen supply and transfer in the reactors, even at higher energy costs (Jackson, 1964; Garcia-Ochoa & Gomez, 2009). Oxygen mass transfer is enhanced by creating high surface area, in the form of bubbles, and by ensuring maximum oxygen concentration gradient. The cost and environmental burden of operating bioreactors may consequently be reduced by changing the aeration method to provide high surface area at lower energy consumption.

Venturi aerators have been reported to consume less energy than conventional airlift reactors, bubble columns and stirred tanks (Jackson, 1964; Rodriguez et al., 2012) mostly because no compressor is needed for the gas. They have also been reported to provide high interfacial areas for mass transfer (Gourich et al., 2007). Venturi aerators are less expensive to install and maintain as they have no moving parts that may break or fail and there is no clogging of gas spargers as with bubble columns (Baylar & Ozkan, 2006).

While it appears that venturi aerators are an easy and obvious solution, there is limited information on their application on an industrial scale. This may be because there are concerns that venturi aerators do not provide enough air in order to avoid oxygen-limiting conditions in reactors. For the operating conditions investigated, oxygen transfer rates in venturi-aerated reactors have been reported to be less than oxygen uptake or utilisation rates required in some biological process such as mineral leaching and aerobic bacterial processes (Bauer, 1963; Rossi, 2001).

In this study energy consumption and oxygen transfer rates in venturi aerated reactors were compared to those in a geometrically similar aerated stirred tank. Oxygen transfer and energy consumption in the venturi-aerated vessel were improved by altering operating conditions and the venturi aerator setup. Applicability of venturi aeration to actual bioprocesses was then tested on an aerobic cultivation of brewer's yeast. Two aeration systems were compared. It is appreciated that oxygen transfer rates obtained in aqueous solutions will most likely differ from those obtained with microbial cultures present.

In presenting the study, the theory and current knowledge governing gas-liquid mass transfer and venturi aeration is provided in Chapter 2. In Section 2.2, measurement of  $k_La$  is reviewed. Sections 2.3 and 2.4 address factors affecting oxygen mass transfer in the stirred tank reactor (STR). Venturi and venture aeration is reviewed in Sections 2.5 to 2.8. Section 2.9 introduces energy considerations of gas-liquid mass transfer. In Chapter 3, the objectives, hypotheses and key questions addressed in the study are put forward. Chapter 4 details the materials and methods used for experiments and the analysis of data gathered from these experiments. The results for both the aerated stirred tank and venturi system are then presented and discussed in Chapter 5, in Sections 5.1 to 5.2 and 5.3 to 5.4 respectively. The study is concluded in Chapter 6 with recommendations on optimisation of a venturi-aerated system also given in the same chapter.

## 2 Literature review

### 2.1 Oxygen mass transfer in bioreactors

Due to the low solubility of oxygen in water (7.5 mg/L at 1 atm and 30 °C) (Liley et al., 1999: 2-127) transfer of oxygen from the gas phase to the liquid phase is often the limiting step in aerobic bioprocesses. In order to analyse this step, Fick's first law can be applied to the diffusion of oxygen from the gas phase to the liquid phase.

The molar flux ( $J_A$ ) of oxygen, denoted by A, into water, B, can be described by Fick's first law for dilute systems given as Equation (2.1). The rate of oxygen transfer  $N_A$  can be found by multiplying the flux by the total surface area,  $A_T$  over which the transfer happens (Equation 2.2).

$$J_A = -D_{AB} \frac{dC_A}{dz} \quad (2.1)$$

$$N_A = -D_{AB} A_T \frac{dC_A}{dz} \quad (2.2)$$

Equation (2.2) can be adapted and applied to the two-film model by Whitman which is applicable to oxygen mass transfer in bioreactors (Villadsen et al., 2011; Noorman, 2006; Kargi & Moo-Young, 1985). Figure 2.1 illustrates the assumptions made in applying two-film theory to oxygen transfer in bioreactors. It is assumed that each bubble in the liquid is surrounded by a very thin gaseous film adjacent to another thin liquid film as shown in Figure 2.1. The bulk air and liquid phases next to these films are well mixed (no concentration gradient) (Wesselingh & Krishna, 2000) and transport in the films only occurs by molecular diffusion.

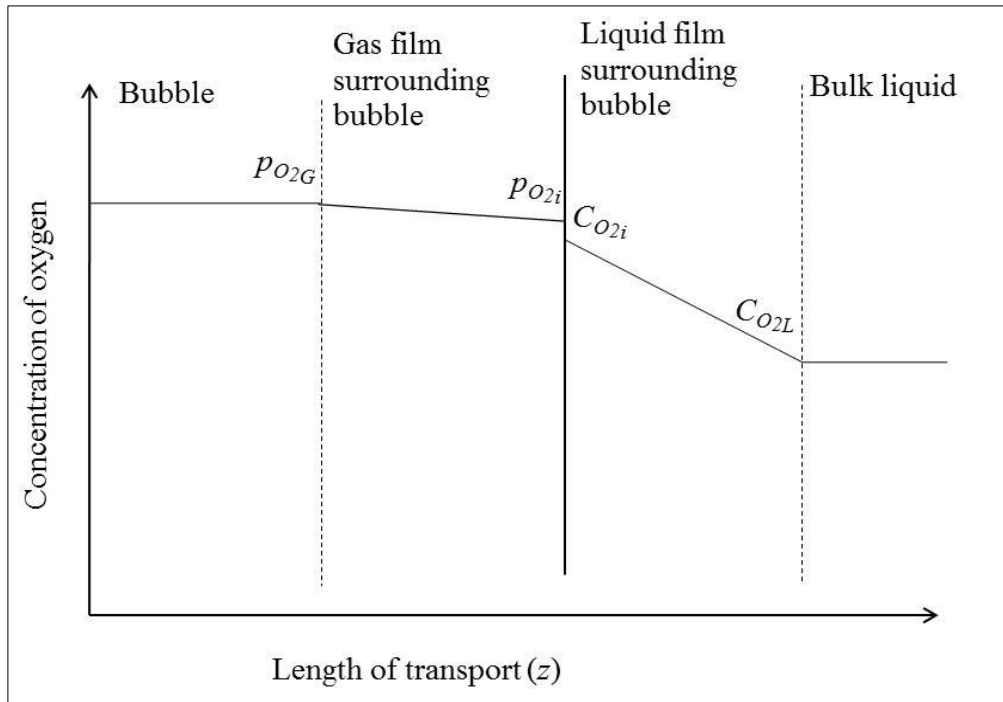


Figure 2.1: Schematic of two-film theory by Whitman

Concentrations on either side of the interface are in equilibrium with each other (Treybal, 1955) and can be related to each other using Henry's law. The rate of oxygen transfer across the interface ( $N_A$ ) is written in terms of the liquid phase and the gas phase in Equation (2.3) and Equation (2.4) respectively. Equations (2.5) - (2.9) show the development of Equation (2.10) which is mostly used to define gas-liquid mass transfer without consumption of the gas.

$$N_A = -k_L A_T (C_{AL} - C_{Ai}) \quad (2.3)$$

$$N_A = -k_G A_T (p_{Ai} - p_A) \quad (2.4)$$

Using Henry's law:

$$p_{Ai} = H_A C_{Ai} \quad (2.5)$$

Combining (2.3) and (2.5)

$$p_{Ai} = H_A \left( \frac{N_A}{k_L A_T} + C_{AL} \right) \quad (2.6)$$

From (2.4)

$$N_A = -k_G A_T \left[ H_A \left( \frac{N_A}{k_L A_T} + C_{AL} \right) - p_A \right] \quad (2.7)$$

Solving for  $N_A$ :

$$N_A = \left( \frac{C_A^* - C_{AL}}{\frac{1}{k_L} + \frac{1}{H_A k_G}} \right) A_T \quad (2.8)$$

$$N_A = K_L A_T (C_A^* - C_{AL}) \quad (2.9)$$

Where

$$\frac{1}{K_L} = \frac{1}{k_L} + \frac{1}{H_A k_G}, \text{ and } C_A^* = \frac{p_A}{H_A}$$

$$\frac{N_A}{V} = k_L a (C_A^* - C_{AL}) \quad (2.10)$$

Resistance to mass transfer in the gas film is much lower than that in the liquid film so  $\frac{1}{K_L}$  is approximated to  $\frac{1}{k_L}$ , giving Equation (2.10). The overall mass transfer coefficient is approximated as the liquid phase  $k_L a$  which is often used to quantify oxygen transfer in mass transfer studies.  $C_A^*$  is the saturation concentration of oxygen in the liquid phase if the liquid phase is in equilibrium with the bulk gas phase at the operating conditions.

## 2.2 Determination of the mass transfer coefficient ( $k_L a$ ) in a stirred tank

The value of  $k_L a$  obtained can depend strongly on the method of measurement used (Gourich et al., 2007; Atkins & Mavituna, 1983). Different methods are used to calculate  $k_L a$  from measurable quantities such as dissolved oxygen concentration and reaction rates. Most of these methods are based on an oxygen mass balance on the liquid phase:

$$\frac{dC_L}{dt} = k_L a (C^* - C_L) - OUR \quad (2.11)$$

where  $C^*$  is determined from the partial pressure of oxygen in the gas phase using Henry's law. Various models are applied to the gas phase in order to determine this partial pressure. The gas phase can be assumed to be a plug or perfectly mixed, with the change in concentration in this gas phase depending on the model (Villadsen et al, 2011; Linek et al., 1987; Ruchti et al, 1981).



### 2.2.1 Sulphite oxidation method

Sulphite is oxidised by oxygen to give sulphate in the reaction:



The rate of sodium sulphite oxidation is measured by titrating samples from the reactor with standard iodide-iodate solution at different times and the amount of sodium sulphite remaining can be determined subsequently. It is accepted that in the presence of a catalyst, the rate of sulphite oxidation is high enough such that the dissolved oxygen (DO) concentration in the reactor remains negligible. If the reaction is fast enough that the reaction is mass transfer limited and oxygen is consumed at the rate at which it is transferred into the liquid phase (Garcia-Ochoa & Gomez, 2009; Villadsen, Nielsen & Liden, 2011) Equation (2.11) becomes Equation 2.13

$$OTR = k_L a (C^* - C_L) = k_L a C^* = \frac{1}{2} \frac{dC_{SO_3^{2-}}}{dt} \quad (2.13)$$

The sulphite method is useful where a dissolved oxygen (DO) electrode may be too slow to record fast changes in concentration, or may influence hydrodynamic properties of some small reactors such as microwells. However, it is not widely recommended because adding a salt can alter the hydrodynamic properties of the liquid and affect the  $k_L a$  value (Garcia-Ochoa & Gomez, 2009; Bandaiphet & Prasertsan, 2006; Gogate & Pandit, 1999). Linek & Vacek (1981) reported that increasing the concentration of sulphite resulted in a reduction in the absorption rate of oxygen into the solution due to the reduced solubility and diffusivity of oxygen in sulphite solutions. Literature on the sulphite oxidation method also varies on the correct sulphite and catalyst concentrations to be used in order to maintain a diffusion-limited reaction without enhancing mass transfer by a reaction. If the reaction is too fast, it will occur in the liquid film, resulting in enhanced mass transfer, thus a higher value for observed  $k_L a$  (van't Riet, 1979). Puskeiler & Weuster-Botz (2005) suggest a  $Co^{2+}$  concentration of  $10^{-3}$  M. The Hatta number (Ha) is a measure of  $k_L a$  enhancement due to chemical reaction and can be used to determine the region in which the reaction is zero order in sulphite concentration (Ruchti et al., 1985). This region can also be found experimentally.

### 2.2.2 Dynamic gassing in method

In the dynamic gassing in method, nitrogen is sparged into the liquid until the DO concentration is zero. Air or oxygen is then sparged into the liquid and the change of DO concentration with time is

measured using an oxygen electrode. If water is used and there are no microorganisms ( $OUR = 0$ ), integrating the mass balance on the liquid phase, Equation ((2.11)), gives Equation (2.14) where  $C_0$  is the initial DO concentration at time  $t_0$ . The  $k_L a$  is the slope of a plot of  $\ln \frac{C^* - C_L}{C^* - C_0}$  against  $(t - t_0)$ . Only the linear portion of this graph is taken into consideration because initially, residual bubbles of nitrogen are still present in the liquid and a change in gas supply may result in a different bubble regime. There is therefore a transition period before a steady surface area is established (Robinson & Wilke, 1973; Ruchti et al., 1981). This method is well documented, widely used and gives accurate values of  $k_L a$  (Garcia-Ochoa & Gomez, 2009; Gourich et al., 2007).

$$\ln \frac{C^* - C_L}{C^* - C_0} = -k_L a(t - t_0) \quad (2.14)$$

In the presence of microorganisms,  $OUR$  can be determined using Equation (2.15) by switching off the oxygen supply and measuring the change in oxygen concentration with time.

$$OUR = \frac{dC_L}{dt} \quad (2.15)$$

Drawbacks to the dynamic method are that a delay in the response of the DO electrode to changes in oxygen concentrations, if not accounted for, will give inaccurate values of the mass transfer coefficient. This delay is caused by a resistance to oxygen transfer around or inside the electrode (Ruchti et al., 1981). The response time constant of an oxygen electrode is the time it takes for the electrode to reach 63% of the final value after a step change (Garcia- Ochoa & Gomez, 2009; Tribe et al., 1995; Van't Riet, 1979). This time should be less than  $k_L a^{-1}$  by a factor greater than ten in order to obtain accurate values (Garcia-Ochoa & Gomez, 2009; Gourich et al., 2008). A DO electrode with response time constant of the same order as  $k_L a^{-1}$  can still be used but the values of  $k_L a$  obtained have to be corrected (Gourich et al. 2008).

Response of a DO electrode can be modelled as first order according to Equation (2.16), in which  $C_m$  is the concentration displayed on the DO meter, while  $C_L$  is the actual concentration of oxygen in the liquid phase and  $\tau_r$  is the response time constant of the electrode (Tribe et al., 1995). Solving Equations (2.16) and (2.11) simultaneously gives Equation (2.17) which accounts for the delay in the DO electrode response and gives more accurate values for  $k_L a$ .

$$\frac{dC_m}{dt} = \frac{C_L - C_m}{\tau_r} \quad (2.16)$$

$$C_m = C_{sat} + \frac{C_{sat} - C_0}{1 - \tau_r k_L a} \left[ \tau_r k_L a \exp\left(\frac{-(t - t_0)}{\tau_r}\right) - \exp(-k_L a (t - t_0)) \right] \quad (2.17)$$

Tribe et al. (1995) used an electrode with a response time of 15 s and found that the error obtained when electrode response was neglected ranged between 10% and 60% for values of  $k_L a$  between 1.8 and 9 min<sup>-1</sup>. Error increased with increasing  $k_L a$ .

In bubble column studies with an electrode with a response time of 7 seconds, Gourich et al. (2008) found  $k_L a$  without accounting for electrode response to be in agreement with the corrected  $k_L a$  at low gas velocities. At higher gas velocities, which correspond to higher values of  $k_L a$  of about 4.5 min<sup>-1</sup>, there was up to 40% difference in the values. It can be noted that the discrepancy is still high even though  $\tau_r^{-1}$  is greater than  $k_L a$  at these conditions.

Correia & Clarke (2009) found no significant difference in the values of  $k_L a$  obtained with or without accounting for response time of the electrode. The response time of the electrode used in their studies is not reported, but it may have been negligibly small.

### 2.2.3 Hydrogen peroxide method

In this method, the rate at which oxygen is transferred from the liquid phase to the gas phase is measured. Hydrogen peroxide decomposes in the presence of catalase according to Equation (2.18) (Villadsen et al, 2011). The rate of reaction is first order in both peroxide and catalase concentration.

Hydrogen peroxide is fed continuously into the reactor at a known rate and concentration of  $Q_{H_2O_2}^f$  and  $C_{H_2O_2}^f$  respectively, and oxygen concentration in the liquid phase ( $C_L$ ) is measured after steady state is reached. The  $k_L a$  can then be calculated using Equation (2.19). Aeration and agitation are kept constant as in the other methods.



$$k_L a (C^* - C_L) = -\frac{1}{2} \frac{Q_{H_2O_2}^f C_{H_2O_2}^f}{V} \quad (2.19)$$

As with the sulphate oxidation method, this method works where a DO electrode response is too slow. However, unlike with the sulphite method, physical properties of water are only altered slightly, and

the product of the reaction is water which may be reused over and over again. The concentration of oxygen in the gas phase has to be known in order to estimate  $C^*$ .

Instead of catalase, Muller & Davidson (1992), Pinelli et al. (2010) and Vasconcelos et al (1997) used  $MnO_2$  as the catalyst and obtained similar results, suggesting that the solid particles did not reduce mass transfer area at the low concentration it was used. Of concern when using this method is that the additional oxygen bubbles generated may result in overstating of  $k_La$  (Muller & Davidson, 1992).

#### 2.2.4 Oxygen balance method

The amount of oxygen transferred to the liquid phase can be determined by measuring amount of oxygen in the inlet and outlet gas streams and in the liquid, and then carrying out a mass balance at steady state as shown in Equation 2.20 (Garcia-Ochoa & Gomez, 2008). The gas volumetric flow rate and concentration are denoted by  $Q_G$  and  $C_G$  respectively. This method requires very sensitive equipment to detect small and fast changes in oxygen concentration.

$$Q_G^f C_G^f - Q_G^e C_G^e = k_L a (C^* - C_L) \quad (2.20)$$

#### 2.2.5 Dynamic pressure method

Gogate & Pandit (1999) and Correia & Clarke (2009) propose that  $k_La$  values reported from the dynamic method may be lower than the actual  $k_La$  values and that dynamic pressure method (pressure step procedure), which is relatively new, is more accurate. This method may be used for aqueous and electrolyte solutions (Correia & Clarke, 2009; Linek et al., 1993). To find  $k_La$  using this method, the pressure of the system is subjected to an upward step change. This increases partial pressure of oxygen in the gas phase. Dynamic pressure method still involves measuring oxygen concentration in the liquid phase after each pressure step change; therefore response time of the oxygen electrode has to be accounted for. The  $k_La$  from dynamic gassing out has been found to be close to the more accurate value obtained from the pressure step when the lag response of the oxygen electrode is taken into account.

The dynamic gassing in method was chosen for the present study because it is simple and easy to conduct, and the delay in the probe response was small enough to give accurate values when corrected for.

## 2.3 Factors affecting oxygen transfer and $k_{La}$ in stirred tank reactors

The rate and extent of mass transfer of oxygen in bioreactors is affected by physical properties of the system under consideration and by operating conditions in the reactor. Oxygen transfer rate can be improved by increasing the concentration gradient ( $C^* - C_L$ ) across the distance over which transport occurs ( $z$ ).  $C^*$  is affected by changing the pressure and temperature of the system because the solubility of oxygen in water changes with temperature and pressure (Dhanasekharan et al., 2005; Welty et al, 2001; Tromans, 1998; Atkinson & Mavituna, 1983). These conditions are generally kept constant when comparing mass transfer rates between reactor systems.

When Equations (2.2) and (2.3) are considered, it can be seen that  $k_{La}$  is affected by the diffusivity of oxygen in the liquid ( $D_{AB}$ ), thickness of the fictitious liquid film through which oxygen diffuses ( $z$ ) and the volumetric surface area across which oxygen is diffusing ( $a$ ). Improving  $D_{AB}$  and  $a$  will result in higher  $k_{La}$ , while increasing the film thickness will give a lower  $k_{La}$ . The diffusivity and concentration gradient of oxygen in the bioreactor are often limited by operating temperature and pressure (Garcia- Ochoa & Gomez, 2009), therefore improving oxygen mass transfer in bioreactors is largely done through maximising mass transfer area and oxygen concentration gradient. The surface area and film thickness cannot be directly measured or controlled in stirred tank reactors; however some operating conditions which are known to affect these variables can be controlled and used to improve  $k_{La}$ .

### 2.3.1 Agitation

The liquid phase can be agitated by mechanical agitators or by air sparging. Impeller agitation significantly increases the volumetric interfacial surface area by creating small bubbles and breaking up large bubbles (Dhanasekharan et al, 2005; McCabe et al., 2001). Reduced bubble size also results in greater gas holdup (Clarke & Correia, 2008; Joshi et al., 1981). Surface area increases with gas holdup according to Equation (2.21) (Villadsen et al., 2011; Gogate et al., 2000).

$$a = 6 \frac{\varepsilon_G}{(1 - \varepsilon_G)D_b} \quad (2.21)$$

Mixing also facilitates a uniform concentration gradient between the liquid and gas phases, thus enhancing oxygen mass transfer rate.

In stirred tank reactors, increasing the agitation rate generally results in increased  $k_{La}$  up to a maximum (Kapic & Heindel, 2006; Peskelier & Weuster-Botz, 2005; Stenberg & Andersson, 1988;

Robinson & Wilke, 1973) and agitation is often limited by the need for energy efficiency as the enhancement of  $k_La$  with agitation is not linearly proportional to the increased energy requirement (Galaction et al., 2004). For comparison purposes, aeration efficiency can be described by Equation (2.22) (Garcia-Ochoa & Gomez, 2008; Rodriguez et al., 2012). Agitation rate is expressed in terms of power input per unit volume of reactor ( $P/V$ ).

$$\text{Aeration efficiency} = \frac{k_La}{E} \quad (2.22)$$

### 2.3.2 Gas flow rate

If the residence time of the gas in the reactor is high, oxygen transfer into the liquid will result in a reduction in the partial pressure of oxygen in the gas phase. This reduces the driving force ( $C^* - C_L$ ) (Villadsen et al., 2011; van't Riet, 1979), resulting in slower mass transfer rates.

At low stirring speeds, an increase in the gas flow rate improves agitation of the liquid phase as well as  $k_La$ . Increased agitation from air flow results in the same benefits as with increased mechanical agitation, though not necessarily to the same degree. Robinson & Wilke (1973) found that doubling the gas flow (0.5 vvm to 1 vvm) in distilled water did not have an effect on  $k_La$  at high agitation rates (600 – 1200 rpm), while Clarke et al. (2006) report that even at high agitation rates, changing the aeration rate impacts  $k_La$  for air flow rates less than 0.7 vvm.

The primary effects of increasing gas flow rate in a stirred tank are therefore improved agitation, volumetric mass transfer area and concentration gradient.

### 2.3.3 Broth composition

Solubility and diffusivity of oxygen in the liquid phase varies depending on the physical properties of the liquid. Some solutes affect the formation and size of bubbles, which in turn determines the interfacial surface area in the reactor (Correia & Clarke, 2009; Gourich et al., 2008; Ratledge & Kristiansen, 2006; Gauthier et al., 1990; Ruchti et al., 1985; Atkinson & Mavituna, 1983). Galaction et al. (2004) compared oxygen mass transfer in a stirred tank for microbial suspensions containing non-respiring cells (*Propionibacterium shermanii*, *S. cerevisiae*, *Penicillium chrysogenum*, mycelial pellets and free mycelia) to simulated broths of the same viscosity with no cells present. They found that biomass accumulation in the reactor caused increased viscosity of the broth and reduction in oxygen solubility, and that reduction in the mass transfer rate was mainly a result of cells blocking the

surfaces of the bubbles, thus reducing mass transfer area. In yeast fermentation, doubling cell concentration from 60 g/l dry weight to 120 g/l dry weight reduced  $k_{La}$  by 25 %. Carboxymethyl cellulose was used to increase viscosity of the broths without cells. Germain et al. (2007) and Bandaiphet & Prasertsan (2006) also found that increased viscosity from biomass concentration gave lower oxygen transfer rates. Furthermore, Galaction et al. (2004) related  $k_{La}$  to power consumption by the impeller. They found that energy efficiency decreased with increased power consumption.

Dissolved components in the reactor also impact oxygen transfer rates. The  $k_{La}$  was  $0.3 \text{ min}^{-1}$  in tap water, and  $0.12 \text{ min}^{-1}$  with 10 wt% molasses. (Deckwer et al., 1974). Similar data are reported by Stieger (1999), relating to the lysine bioprocess by Clarke et al. (2006) and Clarke & Correia (2008) who found that aqueous solutions of hydrocarbons with oxygen in their molecular structure increased  $k_{La}$ . Wilke & Robinson (1973) report that ionic solutions gave higher  $k_{La}$  values than distilled water using the dynamic method, and that the difference was greater at higher agitation rates up to a certain limiting ionic concentration.

Comparison of  $k_{La}$  between systems should therefore take into account these effects. In addition, where mass transfer studies are conducted in media different to that used in a bioreactor, it is valuable to consider how results would be affected by changes in the broth.

## **2.4 Correlation of $k_{La}$ in stirred tank reactors**

*Because the variables have an indeterminate collective effect on gas-liquid mass transfer, one has to be cautious when comparing  $k_{La}$  values obtained in different systems. Figure 2.2 shows results obtained for reactors of different volumes and aeration rates, but similar geometries. Reactor specifications (working volume ( $V$ ), reactor diameter ( $T$ ) and impeller type and diameter ( $D$ )) for these studies are given in*

Table 2.1. The studies were conducted with water in stirred tanks. In the Robinson & Wilke (1973) and Stenberg & Anderson (1988) studies, aeration rate was varied for the different agitation rates.

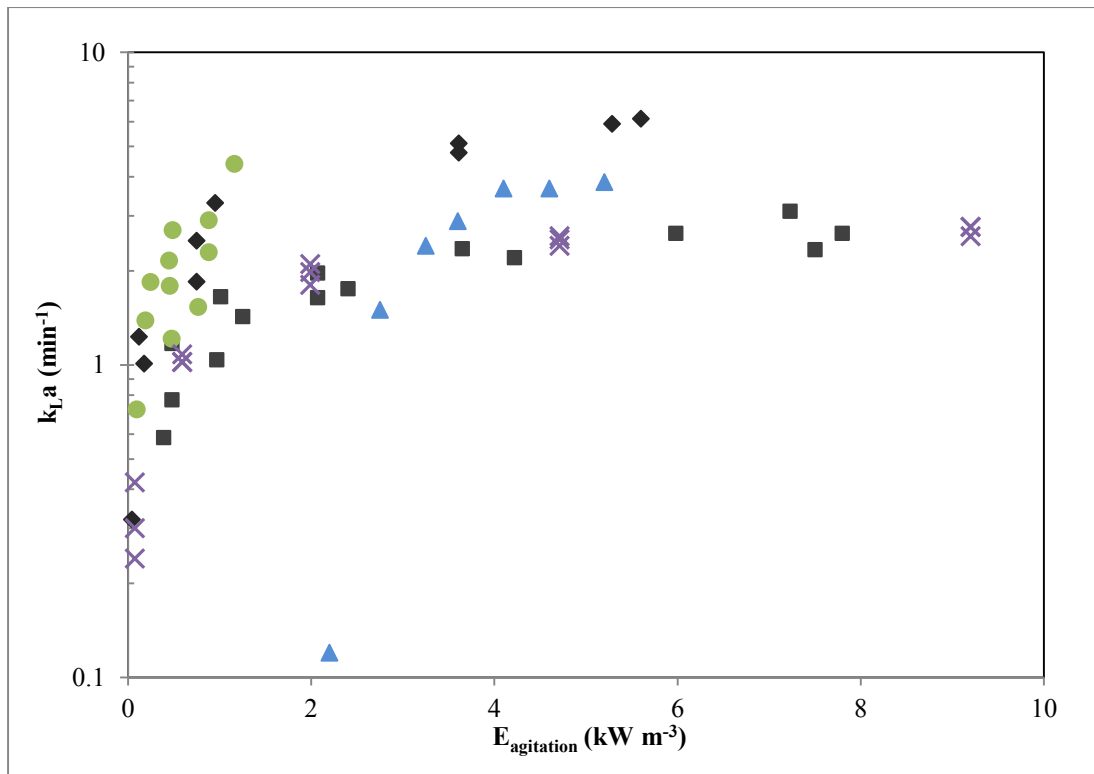


Figure 2.2: Variation of  $k_La$  with agitation power for different studies (Stenberg & Anderson, 1988 ♦; Robinson & Wilke, 1973 ■; Shukla et al., 1999 ▲; Williams., 2005 ×; Chandrasekharan & Calderbank, 1981 ●)



Table 2.1: Reactor specifications for  $k_La$  studies shown in Figure 2.2

Reference	Reactor specifications	Air flow rate (vvm)
Williams (2005)	<ul style="list-style-type: none"> <li>• <math>V = 0.0045 \text{ m}^3</math>, <math>T = 0.18 \text{ m}</math>, <math>H/T = 1</math></li> <li>• 2 Rushton turbine impellers, <math>D = 0.06 \text{ m}</math></li> <li>• Dynamic gassing in method</li> </ul>	1, 1.25, 1.5
Shukla et al. (1999)	<ul style="list-style-type: none"> <li>• <math>V = 0.00512 \text{ m}^3</math>, <math>H/T = 1.19</math></li> <li>• Rushton turbine &amp; Pitched blade downflow impellers, <math>D = 0.074 \text{ m}</math></li> <li>• Dynamic gassing in method</li> </ul>	0.56
Stenberg & Andersson (1988)	<ul style="list-style-type: none"> <li>• <math>V = 0.12 \text{ m}^3</math>, <math>T = 0.54 \text{ m}</math>, <math>H/T = 1</math></li> <li>• Single Rushton turbine impeller, <math>D = 0.178 \text{ m}</math></li> <li>• Dynamic gassing in method</li> </ul>	25, 48
	<ul style="list-style-type: none"> <li>• <math>V = 0.6 \text{ m}^3</math>, <math>T = 0.95 \text{ m}</math>, <math>H/T = 1</math></li> <li>• Single Rushton turbine impeller, <math>D = 0.305 \text{ m}</math></li> <li>• Dynamic gassing in method</li> </ul>	5, 10
	<ul style="list-style-type: none"> <li>• <math>V = 3 \text{ m}^3</math>, <math>T = 1.56 \text{ m}</math>, <math>H/T = 1</math></li> <li>• Single Rushton turbine impeller, <math>D = 0.521 \text{ m}</math></li> <li>• Dynamic gassing in method</li> </ul>	1, 2, 4
Chandrasekharan & Calderbank (1980)	<ul style="list-style-type: none"> <li>• <math>V = 1.43 \text{ m}^3</math>, <math>T = 1.22 \text{ m}</math></li> <li>• Pressure step method</li> </ul>	0.17, 0.36, 0.56
Robinson & Wilke (1973)	<ul style="list-style-type: none"> <li>• <math>V = 0.0025 \text{ m}^3</math>, <math>T = 0.154 \text{ m}</math>, <math>H/T = 1</math></li> <li>• Single Rushton turbine, <math>D = 0.0508 \text{ m}</math></li> <li>• Dynamic gassing in method</li> </ul>	0.5, 15

The results illustrate how widely  $k_{La}$  varies ( $0.6\text{--}3 \text{ min}^{-1}$  at  $0.5 \text{ kW m}^{-3}$ ) even with seemingly similar operating conditions. Although it has been found that the effects of agitation power input on  $k_{La}$  are not affected by stirrer type or number of stirrers for vessels with  $H/D$  close to or less than one (Van't Riet, 1979); dissimilarities among various studies remain.

Despite the variations, it has been agreed that  $k_{La}$  in a laboratory scale stirred tank reactor is related to the gassed power input into the reactor and superficial gas velocity ( $u_G$ ) by Equation (2.23), where  $C_1$ ,  $\alpha$  and  $\beta$  are constants dependent on the reactor under investigation, and  $P$  is the power supplied to the

impeller and  $V$  is the operating volume of the reactor (Garcia-Ochoa & Gomez, 2009; Kapic & Heindel, 2006; Van't Riet, 1979). Schlüter & Deckwer (1992) found that  $k_L a$  was better correlated with aeration rate in units of vvm for comparison of reactors at different scales (72 L to 3000 L).

$$k_L a = C_1 \left( \frac{P}{V} \right)^\alpha u_G^\beta \quad (2.23)$$

Typical values of the constant and exponents for Equation (2.23) in an air- water system are given in Table 2.2. Gogate et al. (2000) report the same ranges as Van't Riet (1979) and suggest that the value of  $\beta$  depends on superficial gas velocity ( $u_G$ ). At high enough  $u_G$ ,  $\beta$  could be as low as 0.2. The correlation only provides loose bounds on variation of  $k_L a$  with agitation power input and aeration rate as indicated by the range of values in Table 2.2.

Table 2.2: Typical values for constants in Equation (2.23) for an air- water system in a stirred tank reactor

$\alpha$	$\beta$	$C_1$	Reference
0.47	0.6	0.04	Kapic & Heindel (2006)
0.59	0.55	0.04	Nocentini et al. (1993)
0.59	0.4	0.00495	Linek et al. (1987)
0.35- 0.5	0.3- 0.6	0.015	Van't Riet (1979)

## 2.5 Principles of Venturi aeration

Venturi aerators are based on the first law of thermodynamics and, for incompressible fluids, can be defined by the Bernoulli equation given by Equation (2.24).

$$\pi + \frac{1}{2} \rho_L v^2 + \rho_L g h = \text{constant} \quad (2.24)$$

Fluid flow is assumed to be steady and heat transfer is negligible (Welty et al., 2001). The narrow throat of the venturi results in increased fluid velocity which corresponds to lower pressure in the throat section. If the pressure drop results in pressure that is lower than atmospheric pressure, air is forced from the atmosphere through the holes in the wall of the neck into the pipe without the need for pumping (Jackson & Collins, 1964; Baylar & Ozkan, 2006). Gas entrained in the liquid is in the form

of finely dispersed bubbles (Bauer, 1963; Cramers, 1992). When the liquid flows through the divergent part of the tube, it reduces speed and regains most of its pressure energy (Bauer et al., 1963).

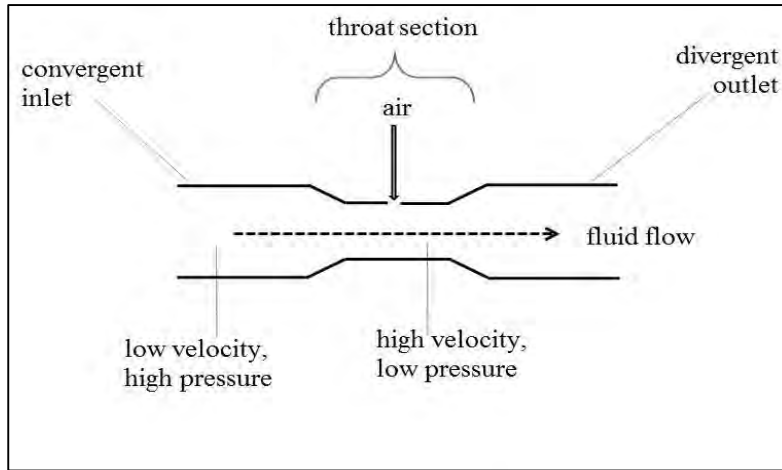


Figure 2.3: Schematic of a venturi device

The amount of gas discharged through a small opening across a pressure drop can be calculated from Equation (2.25), where  $\pi_1$  and  $\pi_2$  are the upstream and downstream pressures of the gas respectively. In the case of the venturi aerator,  $\pi_1$  is atmospheric pressure and  $\pi_2$  is the pressure in the throat of the venturi because air is drawn from the atmosphere into the aerator. The symbols  $C$  and  $A$  the discharge coefficient and cross sectional area of the air hole respectively,  $\gamma$  is the ratio of specific heat of air,  $\rho_{air}$  is the density of air at atmospheric pressure and  $g_c$  is a dimensional constant (Federal Emergency Management Agency, 1989: B-4). Equation (2.25) can be used to estimate the flow rate of air through the venturi air hole from the atmosphere into the venturi throat.

$$Q_G = CA \sqrt{2 g_c \rho_{air} \pi_1 \left( \frac{\gamma}{\gamma - 1} \right) \left[ \left( \frac{\pi_1}{\pi_2} \right)^{\frac{2}{\gamma}} - \left( \frac{\pi_1}{\pi_2} \right)^{\frac{\gamma+1}{\gamma}} \right]} \quad (2.25)$$

Friction in the throat section of the venturi results in an overall pressure drop in the liquid (Baylar & Ozkan, 2006; Jackson 1964; Bauer, 1963). Bauer (1963) reported that the pressure drop tripled from 1.3 kPa to 4 kPa when the liquid flow rate was doubled from 20 L min<sup>-1</sup> to 40 L min<sup>-1</sup>. A higher pressure drop requires a pump with higher capacity to drive liquid through the venturi loop.

Most, if not all, of the gas mass transfer is expected to occur in the divergent outlet and the liquid exiting the venturi is nearly saturated with oxygen (Jackson & Collins, 1964). Bauer et al. (1963)

found that 80% of oxygen transferred to the liquid stream in a venturi aerator was transferred at a distance less than 25 cm away from the air hole in a 80 cm divergent outlet.

### 2.5.1 *Liquid flow rate*

The rate at which liquid is pumped through a venturi device has a considerable effect on oxygen transfer in a water-air system because it determines the amount of air flowing into the venturi (Dong et al., 2012; Baylar & Ozkan, 2006). Dong et al. (2012) found that while increasing liquid flow rate through the venturi increased  $k_{La}$  by 1.5 times, the rate of increase of  $k_{La}$  was lower for higher liquid flow rates. This was attributed to reduced residence time of bubbles in the tank at higher liquid flow rates. Bauer (1963) proposed that the increased turbulence that came with higher flow rates resulted in greater shear stress which disperses the gas into fine bubbles that in turn result in greater mass transfer area.

Increasing liquid flow rate means increasing pressure drop across the venturi (Bauer, 1963) and consequently energy consumption of the pump. This implies that there is a maximum flow rate at which the reactor's energy efficiency is optimal. Excessive velocities could also result in cavitation at the throat of the venturi (Bauer et al., 1963; Jackson, 1964). In addition, an undesirable "annular flow regime", in which a ring of water flows around air core, was observed by Gourich et al. (2008). They found that the annular regime occurred at the lower range of liquid flow rates of up to 480 L/min at an unspecified velocity. On the other hand, Baylar & Ozkan report that the ratio of gas flow to liquid flow ( $Q_G/Q_L$ ) decreases with increasing liquid flow rate after reaching a maximum. Baylar & Ozkan (2006) show that  $Q_G/Q_L$  is higher at smaller pipe diameter for the same liquid volumetric flow rate (higher liquid velocity). They were measuring flow rate of air out of the tank instead of at the inlet of the venturi therefore smaller gas flow rates could mean that more gas was absorbed into the liquid. These findings suggest that a high volumetric liquid flow rate would result in high oxygen mass transfer rates. However, as shown in

Table 2.4,  $k_{La}$  investigations in venturi aeration have mostly been with liquid flow rates less than 1 vvm.

### 2.5.2 *Venturi geometry*

Hydrodynamic studies in venturi aerators have been done to show the effects of liquid flow rate (Briens et al., 1992; Baylar & Ozkan 2006; Gourich et al. 2007; Gourich et al. 2008) and venturi configuration (Thalasso et al., 1995; Gourich et al. 2007; Dong et al. 2011) on oxygen mass transfer. Other studies show that oxygen mass transfer in venturi-aerated systems may be improved by changing the design of the aerator. Properties such as the area of throat (Baylar & Ozkan, 2006;

Jackson & Collins, 1964), the shape of the throat (Batterham et al., 1994) and the size of the divergent and convergent angles (Baylar & Ozkan, 2006) were found to affect mass transfer. The aerator design affects the amount of air drawn into the pipe and consequently mass transfer rate.

If significant oxygen mass transfer happens only in the venturi aerator, optimisation of the aerator design would improve mass transfer considerably. However,  $k_La$  seems to still be strongly influenced by other parameters such as liquid flow rate and hydrodynamics in the tank, as discussed in Sections 2.5.1 and 2.5.3.

### 2.5.3 *Venturi-reactor configuration*

Jackson (1964) and Rodriguez et al. (2012) assumed that most, if not all, of significant mass transfer occurs between the venturi throat and outlet into the tank, suggesting that changes made downstream of the venturi aerator would not affect oxygen mass transfer rates. On the other hand Briens et al (1992) measured  $k_La$  separately in the venturi and in the tank, which they called the bubbling zone, and found that mass transfer occurs in both with  $k_La$  obtained being roughly similar.

Gourich et al. (2008) and Briens et al. (1992) report that liquid flowing down from a venturi into the reactor (downflow) gave higher  $k_La$  than liquid flowing up into the reactor (upflow). In the case of Gourich et al. (2008),  $k_La$  was doubled by changing the direction of flow into the reactor. This could be attributed to the increased residence time of bubbles in the reactor when a downflow configuration is used (Briens et al., 1992). At low liquid flow rates (less than  $1 \text{ L s}^{-1}$ )  $k_La$  also doubled when the liquid level in the tank was doubled (Gourich et al. 2007). In a study carried out with an upflow aeration system, Dong et al. (2011) found that for outlet depths between 20 and 50 cm, the highest  $k_La$  was achieved when the outlet of the venturi was at a depth of 40 cm below the liquid surface. These results could also be due to increased residence time of bubbles in the tank.

Jackson (1964) found that venturi aerators in series with another did not significantly improve mass transfer rates because the liquid became saturated in the first venturi. For a venturi of 7/8 inch internal diameter, Bauer et al. (1963) found not much difference in  $\text{CO}_2$  absorbed 16.7 and 28.8 inches from the throat, owing to this saturation. A second venturi increased pressure loss across the line, which would result in greater power requirement for the pump. Dong et al (2011) confirmed this when no improvement in  $k_La$  was shown for aerators connected in series, but they did find that connecting venturis in parallel improved  $k_La$ . Investigations were at the same total flow, rate, but different venturi aerators were used for the different set-ups and the variations resulting from these differences were not taken into account.

In summary, studies on the connection of the venturi aerator to the reactor indicate that oxygen transfer is not limited to the venturi outlet, but that significant oxygen mass transfer occurs in the tank downstream of the reactor. Oxygen mass transfer in venturi aerated reactors can therefore be improved by optimising mass transfer in the tank.

## **2.6 Application of venturi aeration to bioreactors**

Presently, large scale application of venturi devices as liquid aerators is found in aerobic wastewater treatment (Mohabes & Tanski, 2004; Jateau et al., 2003; Rodriguez et al., 2012; Fakeeha et al., 1999). Venturi aerators are also used in remediation pond aeration (Baylar & Ozkan 2006). This is done both on a small- and a large-scale in aquariums. Venturi devices are also used in gas scrubbers, where the gas is pumped through the venturi and small amounts of liquid are drawn in as droplets (Gourich et al., 2007). Venturi aeration in the aforementioned applications appears successful, but the use of venturi aerators is still not widespread.

Table 2.3 shows that oxygen transfer in venturi-aerated reactors is comparable to that obtained in other types of bioreactors and is, in some cases, sufficient for the bioprocesses indicated. The variation in the values obtained can be attributed to differences in the reactor setup, size and venturi devices used. In their patent application, Batterham et al. (1994) report that venturi aerators required less power than sparged stirred tanks and that oxygen transfer rates obtained were sufficient to sustain bioprocesses, in their case mineral bioleaching. Further description and comparison of venturi systems is given in

Table 2.4.

The general setup of a venturi aerator in a bioprocess is shown in Figure 2.4. A pump is used to circulate liquid through the venturi continuously (Gourich et al., 2008; Dong et al., 2011; Thalasso et al., 1993)

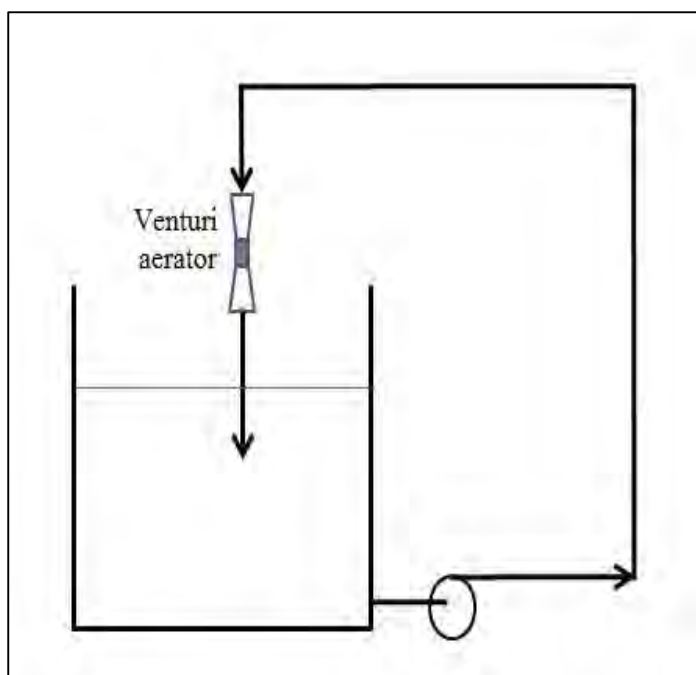


Figure 2.4: Setup of a venturi aerator in a semi-batch process

Table 2.3: Comparison of oxygen transfer in venturi-aerated reactors to sparged reactors

Reference	Aerator type	System	$k_L a$ ( $\text{min}^{-1}$ )	SOTR ( $\text{mg O}_2 \text{ l}^{-1} \text{ h}^{-1}$ )
Rodriguez et al. (2012)	bubble column	water	0.35-0.66	133-190
Dong et al. (2011)	venturi	water	0.14-0.21	76-115
Gourich et al (2007)	venturi	water	2.7	1458
Jackson (1964)	venturi	water	0.1-0.28	47-133
Deckwer (1974)	bubble column	water	9	
Ugwanyi (2008)	Stirred tank	Bacillus in Tanner glucose medium		224-512
Kocabas et al. (2006)	Stirred tank	Bacillus in fructose based medium		260
d'Hugues (1997)	Stirred tank	Chalcopyrite bioleach suspension		1440

## 2.7 Cell damage in venturi aerators

Sparging has been associated with cultured animal cell damage in bioreactors (Chisti, 2000). In some cases, high agitation rates coupled with sparging in stirred bioreactors have resulted in high shear rates close to the impeller, which will damage cells or inhibit cell activity (Bandaiphet & Prasertsan, 2006; Sanchez Perez et al., 2006). Thalasso et al. (1993) report that *A. wieringae* maintained its capacity to metabolize the gaseous mixture of hydrogen and carbon dioxide to acetate for a number of hours even after circulation through a venturi aerator. So far, there have been no reports on studies investigating cell damage due to shear stresses in the venturi. Nevertheless, it is important to consider the possibility.

## 2.8 Measuring $k_La$ in venturi aerated reactors

As in most studies with stirred tanks,  $k_La$  with venturi operation has been determined by performing a mass balance on the concentration of oxygen in the liquid phase, although there are inconsistencies on the models used to describe the system. Results obtained from the various studies are given in

Table 2.4.

Baylar & Ozkan (2006), Fakeeha et al. (1999), and Dong et al. (2011) used the dynamic gassing in method and applied the same equation used for a stirred tank (Equation 2.14).

$$\ln \left( \frac{C^* - C_L}{C^* - C_0} \right) = -(k_L a) t \quad (2.14)$$

Jackson (1964), however, points out that  $k_La$  obtained this way does not have any physical meaning because mass transfer area and concentration change from the tank, through the piping and across the venturi aerator, and can therefore not be represented by one value.

Other investigations considered the mass transfer coefficient across the venturi only, assuming that the significant oxygen mass transfer happens in the venturi (Jackson, 1964; Rodriguez, 2012). Jackson (1964) used Equation (2.26) to find  $k_La$  which was not per unit volume as usually expressed, since they reasoned that area per unit volume is not evenly distributed across the venturi.

$$V \frac{dC_L}{dt} = k_L A_V (C_V^* - C_{V,mean}) \quad (2.26)$$



Instead of a venturi aerator, Pandit et al (1990) aerated liquid in a centrifugal pump that also worked as an air aspirator. They considered mass transfer in both the tank and across the aspirator as described by Equations (2.27) and (2.28). The pump was taken to be a well-mixed CSTR. The concentration of oxygen was measured in the tank and in the stream exiting the pump. Briens et al. (1992) also separated mass transfer in the venturi from that in the tank. The  $k_L a$  was measured from passing of deoxygenated liquid through the venturi and into the tank in a steady-state process.

$$\frac{dC_V}{dt} V_V = F(C_L - C_V) + k_L A_V (C_V^* - C_V) \quad (2.27)$$

$$\frac{dC_L}{dt} = \frac{F}{V_T} (C_V - C_L) + k_L a_T (C_L^* - C_L) \quad (2.28)$$

Rodriguez et al (2012) measured DO concentration in the venturi outlet stream ( $C_V$ ) and in the stirred tank ( $C_L$ ). To find  $k_L a$ , they solved Equations **Error! Reference source not found.** and **Error! Reference source not found.** simultaneously, assuming no mass transfer occurring in the stirred tank and neglecting the contribution of the flow terms. Measurement of  $C_V$  showed that DO concentration in liquid coming out of the venturi aerator was close to saturation after ten seconds, whereas  $C_L$  only reached saturation after more than 500 seconds.

Gourich et al. (2007) modelled the venturi aerator and the tank as a single stirred tank reactor, and the piping section before the aerator to have plug flow with contents having a residence time  $\tau_{plug}$ . The mass balance is shown in Equation (2.29). The flow rate and DO concentration of liquid flowing into the reactor was taken to be the same as the one leaving the reactor time  $(t - \tau_{plug})$ . Again  $k_L a$  does not have a strict physical meaning because volumetric mass transfer area is not spread evenly across the venturi and the tank. The  $k_L a$  and  $C^*$  values were estimated from non-linear regression.

$$\frac{dC_L}{dt} = \frac{F}{V_{ST}} (C_L(t - \tau_{plug}) - C_L(t)) + k_L a_T (C_L^* - C_L) \quad (2.29)$$

The results for the different systems reported are shown in

Table 2.4. These  $k_L a$  values can be compared with literature values of  $k_L a$  for conventional sparged and stirred reactors, but there has been no comparison of  $k_L a$  in a venturi aerated reactor to that in a stirred geometrically identical tank reactor in the same study. Therefore differences in  $k_L a$  arising

from variations in reactor geometry and setup, and dissimilarities in  $k_{LA}$  measurement are not taken into account.

Table 2.4:  $k_{LA}$  values for venturi-aerated systems under various operating conditions

Reference	Operating volume ( $m^3$ )	Liquid flow rate (vvm)	$k_{LA}$ ( $min^{-1}$ )
Rodriguez et al (2012)	0.2	0.17	0.463
Dong , Zhu, Wu & Miller (2011)	2.8	0.0621	0.136
		0.0664	0.168
		0.0771	0.213
Gourich (2007)	0.35	$\approx 1.4$	2.7
Fakeeha et al (1999)	0.0589	0.301	0.72
		0.354	0.87
		0.563	1.45
		0.698	1.97
		0.861	2.17
Jackson & Collins (1964)	66.2	0.0074	0.00356
Jackson (1964)	0.137 - 0.149	0.190	0.28
		0.156	0.20
		0.129	0.17
		0.089	0.10

## 2.9 Energy consumption in bioreactors

Power correlations for stirred tank reactors discussed in (2.4) 2.4 only consider power used to agitate the liquid phase by measuring power input to the impeller (Kapic & Heindel, 2006; Garcia-Ochoa & Gomez, 2009; Van't Riet, 1979) which can be calculated using Equation (2.30), where  $N_{PG}$  and  $D$  are the gassed impeller power number and impeller diameter respectively,  $n$  is the stirrer speed and  $\rho_L$  is the liquid density. It has been found that agitation power input in a stirred tank is lower when gas is present in the system due to the reduced apparent density of the gas-liquid suspension (Garcia-Ochoa & Gomez, 2008). Bouaifi et al. (2001) included energy dissipated to the liquid by expanding gas calculated using Equation (2.31) in their energy calculations. In bubble columns, liquid is agitated by the expansion of sparged gas using Equation (2.31) and this is the power considered in comparisons and correlations (Chisti, 1989). The power input to bubble columns calculated using this equation is in some cases as little as a tenth of agitation power input into a stirred tank (Chisti & Jauregui-Haz, 2002). In both cases, the energy used to compress the gas sparged to the reactors is not typically considered.

$$P = N_{P_G} n^3 D^5 \rho_L \quad (2.30)$$

$$\frac{P}{V} = \rho_L g u_G \quad (2.31)$$

These calculations are sufficient to characterise mass transfer properties of reactors, but neglect the overall cost and environmental impact of operating a bioreactor. In some cases, energy input for gas compression is as much as four times higher than that for stirring (Atkinson & Mavituna, 1983). Harding (2009) and Harding and Harrison (2008, under review) have demonstrated gas compression to be the most significant contribution to energy input into the bioprocess across a range of processes: bioplastic, penicillin and enzyme. It is therefore essential to include this energy when considering total operating cost of the reactor.

Gourich et al. (2007), in studies with reactor volumes of 105-350 L, showed that for the same power input,  $k_L a$  in a venturi aerated reactor was half or less than that obtained by other researchers in bubble columns and rectangular airlifts for energy consumption less than 5000 Wm<sup>-3</sup>. Equation (2.32) was used to calculate energy supplied to the system. The first term on the right hand side is the work done on the flowing water by the pump.  $\pi_1$  is the pressure of the water in the venturi throat and  $\pi_2$  is atmospheric pressure. The water has a density of  $\rho_L$  and travels a vertical distance  $\Delta z$  at a velocity  $u$  at the throat. The second term on the right hand side is energy dissipated to the liquid phase in the tank by gas expanding from a pressure of  $\pi_{1gas}$  to  $\pi_{2gas}$ . By measuring the pressure of the water at the throat of the venturi, any frictional losses upstream of the throat are neglected.

$$E = \frac{Q_L}{V} \left[ \pi_1 - \pi_2 + \frac{1}{2} \rho_L u^2 + \rho_L g \Delta z \right] + \frac{Q_G}{V} [\pi_{1gas} - \pi_{2gas}] \quad (2.32)$$

Rodriguez et al. (2012) attained three times more oxygen transfer per unit energy expended in a venturi-aerated reactor than that in a tank with a membrane diffuser. Their experiments were conducted in the same reactor to eliminate variations introduced by differences in reactor geometry and other experimental procedures. Power input to the pump and compressor were calculated using Equations (2.33) and (2.34) respectively. This is the only mass transfer study found so far to account for energy used to compress gas from atmospheric pressure to a higher pressure in the gas supply line. This may also contribute to the results in favour of venturi. Equation (2.34) is also given by Boyce (1999) for calculating energy needed to compress a gas adiabatically.

$$P_{water\ pump} = Q_L (TDH) W \quad (2.33)$$

$$P_{gas\ compressor} = \frac{w \cdot R \cdot T}{K} \left[ \left( \frac{\pi_2}{\pi_1} \right)^K - 1 \right] \quad (2.34)$$

Correlating the  $k_{La}$  with power supplied to agitate the liquid in a reactor is useful to quantify the energy efficiency of a reactor, but the total energy input is an essential parameter to consider when focusing on the cost and environmental impact of bioreactors.

### 3 Hypothesis and key questions

Aerated stirred tank reactors have been used successfully in most aerobic bioprocessing operations, but have high energy input for agitating and aerating the culture, with compression of air requiring a significant portion of the total energy input. Venturi aerators are potentially a less energy-intensive alternative to the mechanical agitation and air compression required in aerated stirred tanks. This is because agitation and air bubbles are supplied by liquid being circulated in the bioreactor. In the reviewed literature, venturi aerators have been shown to require much less energy input than aerated stirred tanks for the same  $k_{La}$  values for the conditions investigated, although investigations have been at low  $k_{La}$ .

The flow rate of the liquid circulated through the venturi and bulk fluid movement in the tank influence the rate of mass transfer in a venturi-aerated bioreactor, with  $k_{La}$  increasing with liquid flow rate. Most studies have only investigated flow rates less than 1 vvm (volume of liquid circulated per total liquid volume per minute) which could explain why mass most transfer rates reported for venturi-aerated reactors have been lower than those in aerated stirred tanks. Furthermore, the comparisons in energy input in the STR and venturi systems have been across different systems and neglected energy used for compression of air in stirred tanks, not required in the venturi. Differences in  $k_{La}$  resulting from varying reactor geometries as well as measurement methods and data analysis have not been considered across the comparisons.

Consequently, it would be useful to use identical tanks and the same analytical methods to compare mass transfer between the STR and venturi systems, and to account for the full energy input, including gas compression, in that comparison. Investigation of  $k_{La}$  in a venturi-aerated reactor at liquid flow rates higher than 1 vvm would show whether mass transfer in these systems has previously been limited by the liquid flow rate.

Oxygen mass transfer rates in microbial cultures with active cells are likely to deviate from those obtained in water; therefore the adequacy of venturi aerators in an aerobic bioprocess should be investigated. Additionally, the higher liquid flow rates result in additional shear stresses in the venturi aerator. For that reason, the viability of cells that have been passed through a venturi aerator must be explored.

### **3.1 Hypothesis**

The venturi-aerated reactor is a promising energy efficient alternative to the conventional sparged stirred tank bioreactor since the required energy consumption is lower in a venturi-aerated reactor than that in a conventional sparged stirred tank reactor for the same volumetric mass transfer coefficient.

### **3.2 Key questions**

- How does  $k_La$  and the associated gas-liquid transfer rates obtained by venturi aeration compare with those in a sparged stirred tank?
- What are the effects of different venturi-reactor configurations?
- How is gas-liquid mass transfer affected by liquid flow rate through the venturi?
- Does all gas-liquid mass transfer in the venturi aerated reactor occur in the venturi recycle loop or is some attributed to fluid dynamics in the tank?
- Is venturi aeration at high liquid flow rates more energy-efficient than conventional aeration?
- Can a venturi aerator be used to obtain adequate OTRs to support processes in bioreactors?
- How do shear rates in the venturi device affect cell activity?

## 4 Materials and Methods

### 4.1 Experimental set-up

#### 4.1.1 Stirred tank reactor

All experiments were carried out for an air-water system at room temperature and atmospheric pressure of  $101.3 \pm 1$  kPa in an open cylindrical plastic vessel as shown in Figure 4.1, with dimensions shown in Table 4.1. The vessel was fitted with a ring sparger (not shown) of the same diameter as the impeller, placed at the bottom of the vessel, below the impeller. The sparger had 6 evenly distributed 1 mm holes facing up and was sealed at one end. Room temperature was  $20 \text{ }^{\circ}\text{C} \pm 2$   $^{\circ}\text{C}$  and did not vary significantly during a single run.

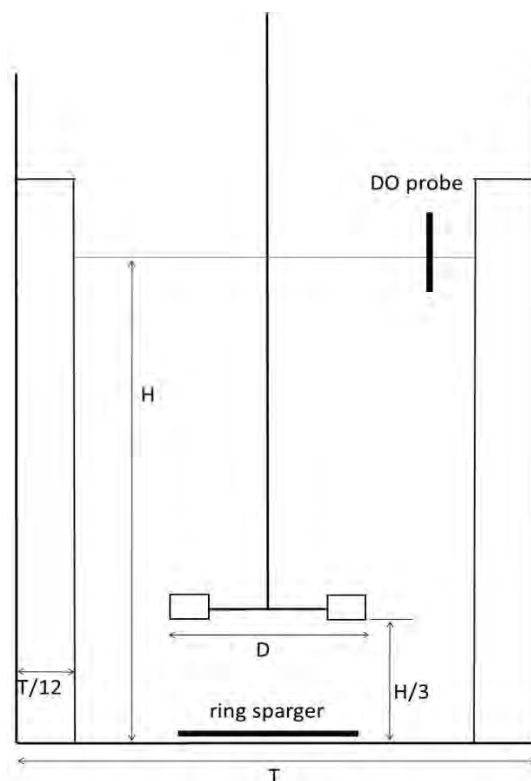


Figure 4.1: Schematic of reactor used in stirred tank experiments

To ensure that the ratio of the vessel diameter: liquid height was equal to 1, 16.3 L of Millipore deionised water was used in the experiments. The  $k_L a$  was measured for this tank at different agitation rates and aeration rates. Agitation rates used and corresponding power input are listed in Table 4.2 . For each of these agitation rates, air was sparged at rates of 0, 12, 16.5 and 25 L min<sup>-1</sup>. The power input to the agitator was calculated from correlations based on the impeller type and Reynolds number in the reactor. The details for power calculations are given in Section 4.4. A Rushton turbine attached

to a Rexon 14'' drill press was used to agitate the liquid. The agitation rate was varied by changing the arrangement of fan belts on the motor of the press and measured optically by a Veeder-root tachometer, model 611. At each setting, the agitation rate varied by less than 5% at the different air flow rates. There were three repeats for each agitation and aeration rate.

*Table 4.1: Dimensions of reactor used in stirred tank experiments*

Diameter, T (m)	0.275
Height of reactor (m)	0.405
H/T	1
Height of liquid in reactor, H (m)	0.275
Operating volume, V (L)	16.3
D/T	0.33
Impeller diameter, D (m)	0.122
Impeller clearance (m)	0.0917
Number of baffles	4
Baffle spacing (m)	0.216
Baffle width (m) (T/12)	0.0229
Sparger diameter (m)	0.275

*Table 4.2: Agitation rates and corresponding power consumption*

Agitation rate (rpm)	Corresponding calculated agitation power ( $\text{Wm}^{-3}$ )
364	509
460	1027
550	1755
688	3435
836	6163

#### 4.1.2 Venturi system

The same vessel used in stirred tank experiments was used in the venturi aeration studies with the set-up shown in Figure 4.2. Two venturi aerators, a Mazzei model 684 injector (Aerator 1) and a Mazzei



model 384 injector (Aerator 2), were used in these experiments. Water was pumped around the circuit using a KM-160 centrifugal pump connected to a Delta Electronics inverter (Model VFD007EL23A), allowing for variable flow rate. Components were connected with reinforced rubber tubing of 20 mm ID. The total liquid volume was maintained at 16.3 L, with liquid in the tank making up about 75% of the total volume. The temperature was maintained at  $20\text{ }^{\circ}\text{C} \pm 2\text{ }^{\circ}\text{C}$  by pumping the solution from the vessel through a 20 mm ID copper coil immersed in a cooling bath as shown in Figure 4.2.

The  $k_La$  was measured for an air-water system for the following setups:

- Setup 1: Aerator 1
- Setup 2: Aerators 1 and 2 in parallel. The two venturi outlet streams were not combined before entering the tank.

In each case, dissolved oxygen concentration as a function of time was determined in the vessel for varied flow rates of liquid pumped through the venturi. For Setup 1, DO concentration was also determined 15 cm downstream of the venturi throat. For each flow rate, venturi outlet heights of 4 cm, 8 cm and 12 cm were used, except in the setup with venturi aerators in parallel, where only the 8 cm height was investigated. The outlet height was measured from the bottom. Positions of the DO electrodes, suction pipe and outlet pipe were kept as much in the same position as possible. The DO electrode in the tank was kept at a third of the liquid depth. The air flow rate through the air hole in Setup 1 was measured by a flowmeter connected to the air hole.

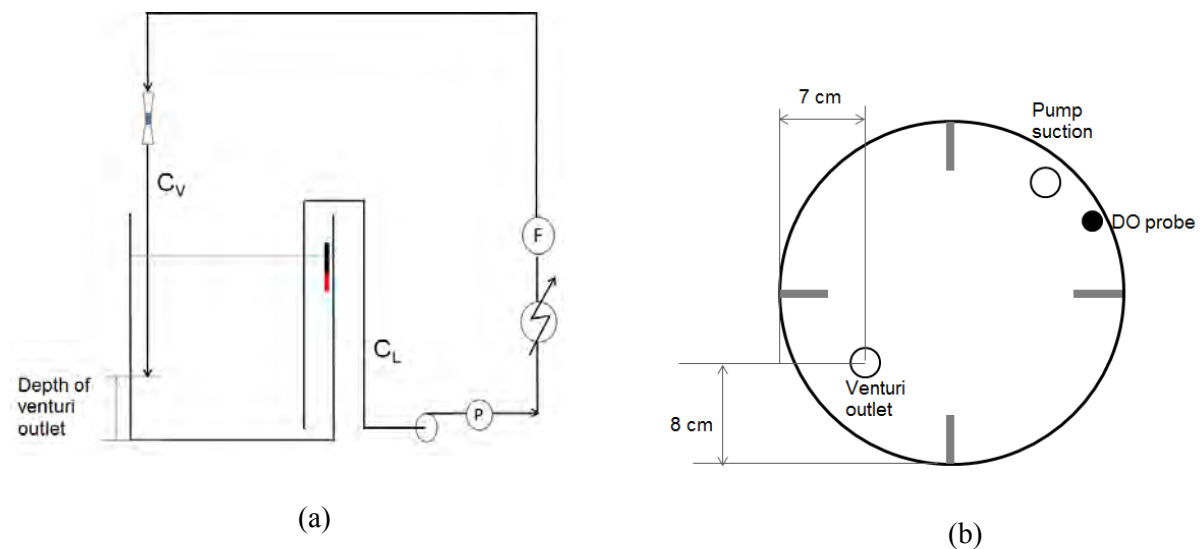


Figure 4.2: Schematic of experimental set-up for venturi aeration experiments (a) shows arrangement of apparatus and (b) shows top-down view of components in the tank

#### 4.1.3 Oxygen measurement equipment

DO in the vessel was measured and logged using an optical Thermo Scientific Orion Star RDO electrode connected to a Thermo Scientific Orion Star A323 RDO/ DO meter. The electrode was calibrated daily. The response time constant of the electrode ( $\tau_r$ ) was 18 seconds, measured by zeroing the electrode in a saturated solution of  $\text{Na}_2\text{SO}_3$ , then immediately transferring the electrode into an oxygen saturated solution and recording the change in DO concentration with time. Using Equation (2.16) to model the electrode response,  $\tau_r$  was determined from measured DO:

$$\frac{dC_m}{dt} = \frac{C_L - C_m}{\tau_r} \quad (2.16)$$

This value was also confirmed by directly measuring the time it took for the reading on the DO meter to be 63 % of the saturated water value after a step change as indicated in literature (Van't Riet, 1979; Garcia- Ochoa & Gomez, 2009; Tribe et al., 1995). Measurements were carried out at different agitation and air flow rates, and it was found that the electrode response was constant for different operating conditions, indicating that the major resistance to mass transfer was internal to the electrode.

The General Electric DOOPT20 instrument was used to measure DO at the venturi outlet, 15 cm downstream of the throat. The instrument has a DOOPT microelectrode with a response time of 4 seconds

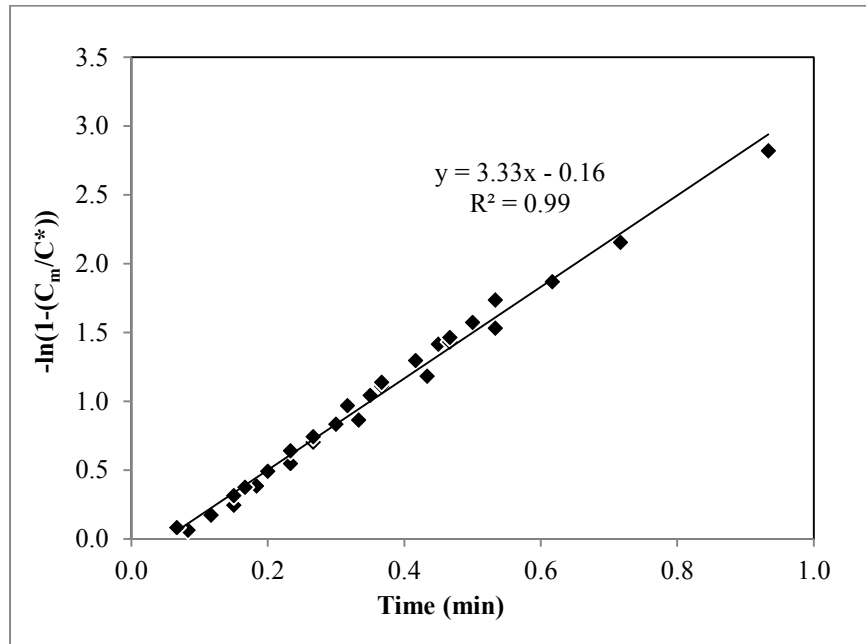


Figure 4.3: Results obtained in the determination of  $\tau_r$ . The reciprocal of the slope of the trend line gives electrode response time in minutes.

## 4.2 Dynamic method for measurement of oxygen transfer

The dynamic gassing in method, described in Section 2.2.2, was used to determine  $k_{La}$  in both the stirred tank and venturi aerated tank due to its speed and simplicity. The greatest source of error was the delayed electrode response. This was accounted for using a first order response model, discussed in detail in Section 4.2.3.

### 4.2.1 Dynamic method in the stirred tank reactor

Liquid in the reactor was deoxygenated by sparging nitrogen into the reactor until the reading on the DO meter was close to zero. The nitrogen flow was then switched off and air flow immediately switched on at a set flow rate and change of DO concentration in the liquid phase was measured and logged using the DO meter.

### 4.2.2 Dynamic method in the venturi-aerated reactor

As in the stirred tank, the liquid phase was deoxygenated using nitrogen gas. Nitrogen was fed through the venturi air hole until DO concentration was close to zero. The nitrogen feed pipe was then removed from the air hole, and air was allowed to flow freely through it. Increase in DO concentration in the liquid was then measured and recorded by the meter.

### 4.2.3 Analytical method for $k_{La}$ determination in the stirred tank

Equation (2.14) is the solution to the mass balance shown in Equation (2.11) with no oxygen consumption. Using the least squares method, the error between  $C_L$  measured by the electrode and  $C_L$  predicted by the mass balance is minimised by solving for  $k_{La}$  in the mass balance.  $C^*$  was calculated from Henry's Law with Henry's constant ( $1.3 \times 10^{-3} \text{ mol L}^{-1} \text{ atm}^{-1}$ ) obtained from Liley et al. (1999). For each set of operating conditions, three runs were conducted and standard deviation from the mean evaluated.

$$\frac{dC_L}{dt} = k_L a_T (C^* - C_L) \quad (2.11)$$

$$\ln \frac{C^* - C_L}{C^* - C_0} = -k_L a(t - t_0) \quad (2.14)$$

Figure 4.4 and Figure 4.5 are examples of how the measured DO changed with time when sparging air into the reactor for each repeat at low agitation and high agitation rates respectively. Also shown is the DO concentration when the lag in probe response is accounted for as given by Equation (4.1), and how the mass balance model used to solve for  $k_L a$  (Equation (2.14)) fits the data. Experiments at other experimental conditions show similar results.

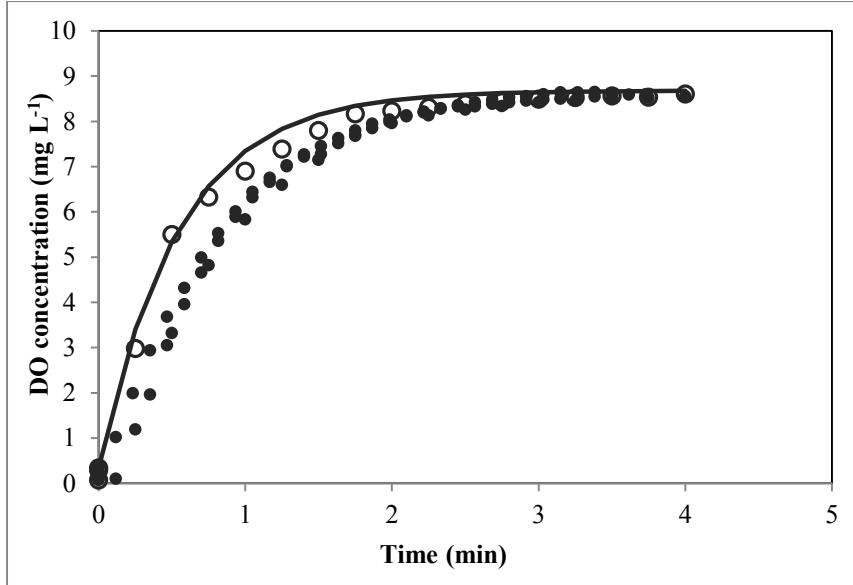


Figure 4.4: Change of DO concentration in the tank with time at agitation power of  $0.509 \text{ kW m}^{-3}$  and  $25 \text{ L min}^{-1}$  for: three repeats as measured by the electrode ( $\bullet$ ); measurements corrected for delay in probe response for one repeat ( $\circ$ ) and DO concentration as predicted by the mass balance in Equation 2.14 for one repeat ( $\text{—}$ )

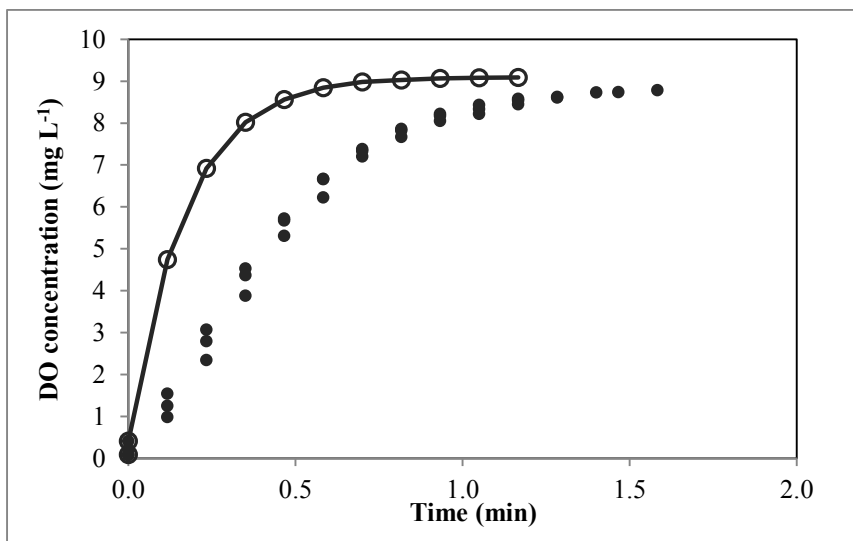


Figure 4.5: Change of DO concentration in the tank with time at agitation power of  $15.36 \text{ kW m}^{-3}$  and aeration rate of  $12 \text{ L min}^{-1}$  for: three repeats as measured by the electrode ( $\bullet$ ); measurements corrected for

delay in probe response for one repeat (○) and DO concentration as predicted by the mass balance in Equation 2.14 for one repeat (—)

#### 4.2.4 Accounting for lag in electrode response

The DO electrode response time was measured to be 0.3 minutes. It was therefore expected that  $k_La$  measurements of  $3 \text{ min}^{-1}$  or greater would be inaccurate. Lag in electrode response is corrected for using Equation (2.16). Figure 4.6 confirms the need to account for electrode response at the values of  $k_La$ . Solving Equation (2.16) for  $C_L$  and using recorded DO concentration data ( $C_m$ ) gives an approximation of the actual DO concentration in the liquid ( $C_L$ ) given in Equation (4.1).

$$\frac{dC_m}{dt} = \frac{C_L - C_m}{\tau_r} \quad (2.16)$$

$$C_L = C_m + \tau_r \frac{dC_m}{dt} \quad (2.16)$$

$$C_{L,n} = C_{m,n} + \tau_r \left( \frac{C_{m,n+1} - C_{m,n-1}}{2 \Delta t} \right) \quad (4.1)$$

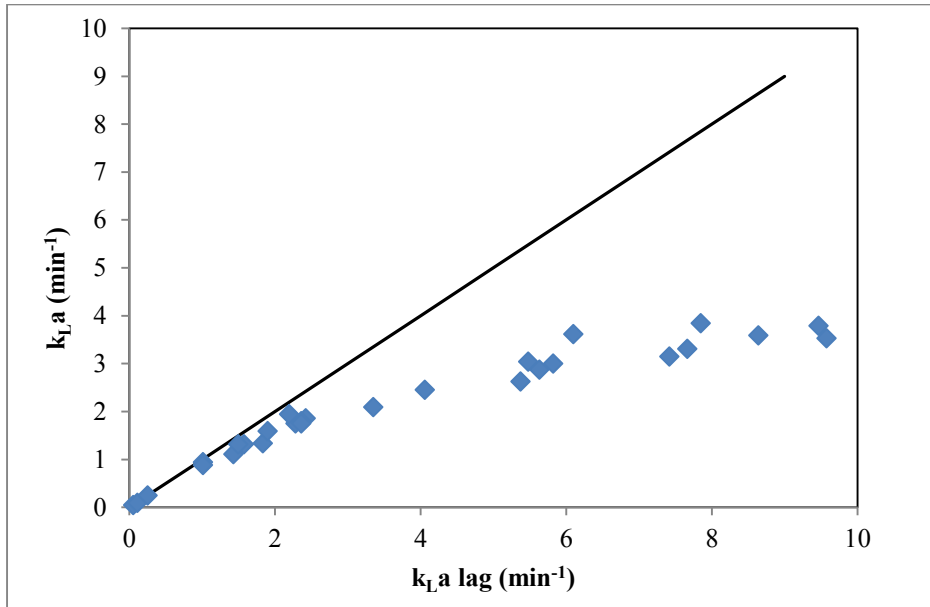


Figure 4.6: The difference between  $k_La$  calculated with electrode response accounted for ( $k_La$  lag) and  $k_La$  measured (no correction) in the stirred tank. The straight line represents the parity line where  $y=x$ .

#### 4.2.5 Analysis of venturi aerated reactor

For comparison between the stirred tank and venturi system, Equation (2.14) from the dynamic method was also used to calculate  $k_L a$  in the venturi-aerated system. Figure 4.7 shows how the model from Equation (2.14) fits DO concentration corrected for the delay in electrode response for one repeat.

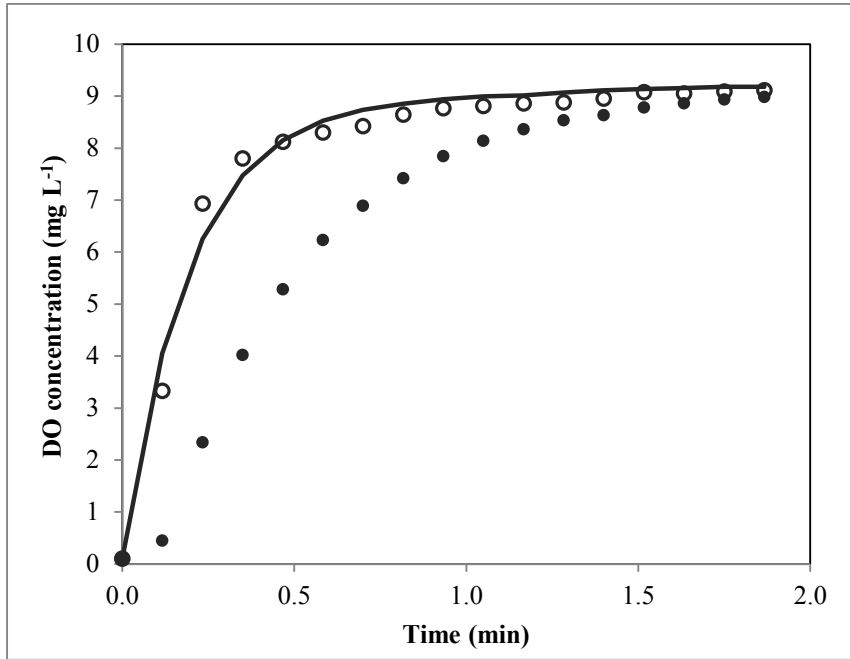


Figure 4.7: Change of DO concentration in the tank for the venturi system with time as: measured by the electrode (●); corrected for delay in probe response (○) and predicted by Equation 2.14 (—) at liquid flow rate of  $42 \text{ L min}^{-1}$  and 8 cm outlet height. The measured values show the average of 3 repeats.

The mass balance used in the dynamic method, however does not strictly apply to venturi aeration because aeration starts in the venturi, which does not have the same mass transfer coefficient as the rest of the tank. Other researchers (Rodriguez et al., 2012 & Jackson, 1964) have applied this equation to just the venturi device and assumed that all mass transfer happens in the venturi. This is inaccurate for this system because many small bubbles formed in the venturi and were observed to be transferred to the tank. Mass transfer equations should therefore take into account the different conditions in the tank and in the venturi aerator.

A mass balance on oxygen in the liquid phase across venturi aerator and across the tank resulted in Equations (2.27) and (2.28):

$$\frac{dC_V}{dt} V_V = F(C_L - C_V) + (k_L A)_V (C_V^* - C_V) \quad (2.27)$$

$$\frac{dC_L}{dt} = \frac{F}{V_T} (C_V - C_L) + (k_L a)_T (C_L^* - C_L) \quad (2.28)$$

$$\frac{dC_V}{dt} \tau_V = (C_L - C_V) + \frac{k_L A_V}{F} (C_V^* - C_V)$$

If the volume of the venturi aerator is much smaller than that of the tank and the liquid flow rate is high enough such that  $\tau_V \ll 1$  then:

$$(C_V - C_L) = \frac{k_L A_V}{F} (C_V^* - C_V)$$

$$C_V = \frac{k_L A_V C_V^* + F C_L}{F + k_L A_V} \quad (4.2)$$

Substituting Equation (4.2) into the stirred tank mass balance, given in Equation (2.28)

$$\frac{dC_L}{dt} = \frac{F}{V_T} \left( \frac{k_L A_V C_V^* + F C_L}{F + k_L A_V} - C_L \right) + k_L a_T (C_L^* - C_L)$$

Solving this equation with initial condition  $C_L = C_0$  at  $t = 0$

$$C_L = \left( C_{L,0} - \frac{\alpha}{\beta} \right) e^{-\beta t} + \frac{\alpha}{\beta} \quad (4.3)$$

where  $\alpha = \frac{F}{V_T} \left( \frac{k_L A_V C_V^*}{F + k_L A_V} \right) + k_L a_T C^*$  and  $\beta = k_L a_T - \frac{F}{V_T} \left( \frac{F}{F + k_L A_V} - 1 \right)$

Results were analysed using Equation (4.3) in order to evaluate mass transfer in the venturi aerator and the tank and better understand the mass transfer characteristics of either separately.

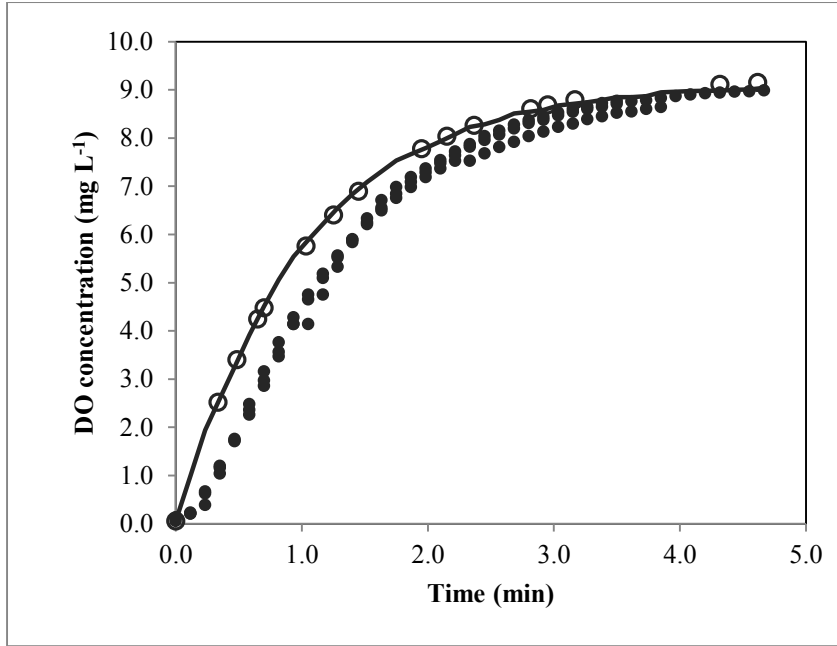


Figure 4.8: Change of DO in the tank with time: as measured by the electrode (●); corrected for electrode response (○) and predicted from the mass balance in Equation (2.28) (—) for a venturi aerated reactor at liquid flow rate of  $22.2 \text{ L min}^{-1}$  and 4 cm outlet height.

Where Equation (2.11) was used for comparison between the stirred tank and the venturi aerated system,  $k_L a$  was regarded as a constant factor quantifying the differences in mass transfer characteristics of the two systems..



### 4.3 Mixing studies in venturi aerated reactor

Mixing studies were carried out in the venturi aerated system. An aliquot of 5 mL of 10.8 M NaCl was injected through the venturi air hole while the pump was running, then the change of conductivity of the solution in the bucket with time was measured. Mixing time was recorded as the time it took from injection to establishing a steady conductivity reading. A steady reading was taken as that when conductivity varied by less than 5% of final values, and these steady values were achieved at most 10 seconds after injection of the salt solution for all experimental setups. An AZ benchtop meter (model 86555) was used to measure conductivity. Measurements were recorded every second by a data logger.

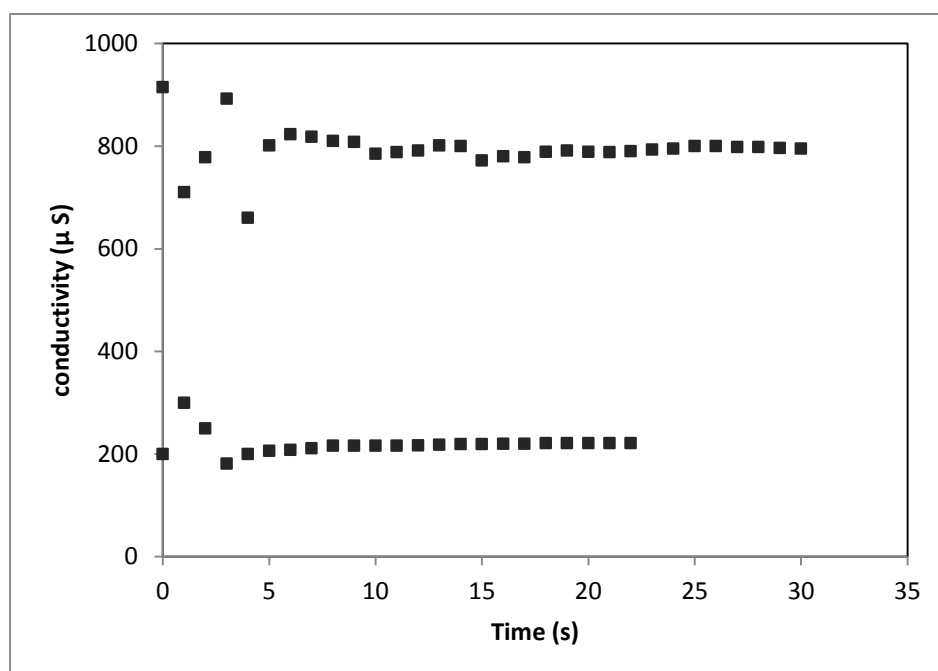


Figure 4.9: Change of conductivity with time after injecting salt for two repeats at a liquid circulation rate of  $22.2 \text{ L min}^{-1}$  at an outlet height of 4 cm

### 4.4 Calculation of power

As discussed in Section 2.9, evaluation of power input to stirred tanks is often limited to power supplied for liquid agitation which can be determined using Equation (2.30) (Sinnott, 2005:473). Correlation of impeller type to power number and Reynolds number is also provided by Sinnott (2005:475) and is used to find the power number.

A substantial motive for introducing venturi aeration is the potential reduction of energy input to the bioreactor by eliminating the need for gas compression prior to sparging the reactor (Jackson, 1964). Therefore, in addition to agitation power, energy used to compress air fed to the reactor

adiabatically was considered to determine the total power supply to the stirred tank. Equation (2.34) was used to calculate power used in compressing the gas, assuming 100% efficiency of the compressor. The pressure of the gas before and after compression is  $\pi_1$  and  $\pi_2$  respectively,  $w$  is the mass flow rate of air,  $\gamma$  is the ration of specific heat capacity of air,  $R$  is the universal gas constant and  $T$  is the temperature of the gas at the compressor outlet, which was taken to be the average atmospheric temperature.

$$P_{agitation} = N_{PG} n^3 D^5 \rho \quad (2.30)$$

$$P_{gas\ compressor} = \frac{\gamma \cdot w \cdot R \cdot T}{K(\gamma - 1)} \left[ \left( \frac{\pi_2}{\pi} \right)^{\frac{\gamma-1}{\gamma}} - 1 \right] \quad (2.34)$$

Energy supplied to the venturi aerated system was taken to be energy supplied to flowing water by the pump. The total dynamic head (TDH) was taken as the discharge pressure of the pump. Therefore energy lost to friction was still included in power supply to the reactor.

$$P_{water\ pump} = Q_L(TDH)W \quad (2.33)$$

The specific power input (P/V) was obtained by dividing the value of the power input calculated (P) by the operating volume of the reactor (V). These calculations are sensitive to operating conditions, and improving operating conditions, for example reducing friction in piping, could significantly affect results. Both sparged stirred tank and venturi aeration energy calculations depend heavily on assumptions made. If air was compressed to 3 bar, power input would increase significantly. The assumptions made for power calculations in this study were:

- Air is compressed adiabatically from atmospheric pressure to 2 bar
- The compressor works at 100 % efficiency

#### 4.5 Aerobic cultivation of Baker's yeast

To test the potential for the venturi- aerated reactor to support rapid yeast growth, the aerobic growth of *biomass* in a venturi aerated reactor inoculated with *S. cerevisiae* was compared to that in an aerated stirred tank at a similar oxygen transfer rate and time period. Brewer's yeast was grown in the reactors according to the experimental method described by van Hille et al. (2014). The reactors were not sterile, therefore other faster-growing microorganisms may have ended up present in the reactors.

At the end of the aerated stirred tank growth experiments, the cells were circulated through the venturi for differing lengths of time, prior to inoculation (10 % volume) into shake flasks to investigate viability and metabolic activity (vitality) of cells that have passed through a venturi aerator several times. One shake flask was inoculated with cells that had been circulated through the venturi-aerated reactor for fifteen minutes, and another with cells that had been in the venturi-aerated reactor for ninety minutes. The control was inoculated with cells that had not been through the venturi.

#### 4.5.1 *Microorganism and culture maintenance*

The stock culture of *S. cerevisiae* was on a YPD agar slant. The original culture was a Brewers' yeast obtained from South African Breweries. A pre-inoculum culture was prepared from this stock culture in 160 mL of medium containing 10 g/L glucose, 5 g/L peptone, 3 g/L yeast extract and 3 g/L malt extract. This culture was cultivated in a 500 mL shake flask at 30 °C and 125 rpm on an orbital shaker. After 24 hours it was transferred to a 5 L shake flask to make the inoculum. The inoculum had 20 g/L glucose, 20 g/L peptone and 10 g/L yeast extract. It was cultivated for 14 hours at 30 °C and 125 rpm on an orbital shaker. The same nutrient concentrations were used in the reactors.

#### 4.5.2 *Operating conditions*

The venturi- aerated reactor was inoculated with the culture described above and operated at a liquid flow rate of 28.2 L/min. The venturi outlet height was 8 cm and  $k_{La}$  in water was  $3.98 \text{ min}^{-1}$ . At these conditions, OTR would be sufficient for yeast growth and shear rates in the venturi aerator were expected to be low enough not to cause damage to the yeast cells. The air drawn into the venturi aerator was not filtered therefore the operation was not sterile. All the experiments were done in duplicate.

The aerated stirred tank was operated at a stirrer speed of 688 rpm ( $3435 \text{ W m}^{-3}$ ) and aeration rate of  $16.5 \text{ L min}^{-1}$ , which gave a  $k_{La}$  of  $5.37 \text{ min}^{-1}$ . The air sparged to the reactor was unfiltered.

For the shake flask experiments, 16 mL culture was inoculated into 144 mL of media in a 500 mL shake flask. The flasks were placed on an orbital shaker at 125 rpm

#### 4.5.3 *Cell growth analysis*

To determine dry weight concentration, 2 mL of the cell culture were pipetted into pre-weighed 2 mL Eppendorf tubes. Each tube was centrifuged and the supernatant decanted into different Eppendorf tubes for glucose analysis. Distilled water was added to the remaining cell pellets, the cells re-suspended and then centrifuged again. The supernatant was decanted and the cells in the Eppendorf tubes dried in an 80 °C oven for 48 hours and then weighed again. The maximum specific growth rate

was calculated from the average growth rate during the exponential phase using Equation (4.4) where  $x_1$  and  $x_2$  are the biomass dry weight concentrations at time  $t_1$  and  $t_2$  respectively.

$$\mu_{max} = \frac{\ln x_2 - \ln x_1}{t_2 - t_1} \quad (4.4)$$

#### 4.5.4 Glucose analysis

Supernatant from centrifuged samples was analysed for glucose. The glucose concentration was measured colorimetrically using the DNS method. The DNS solution contained 10 g/L dinitrosalicylic acid, 0.5 g/L sodium sulphite and 10 g/L sodium hydroxide in deionised water. This solution was added in equal proportions, 0.5 mL in this instance, to the sample. The mixture was then heated for 10 minutes at 90 °C. Under a fume hood, 0.17 mL of 40% potassium sodium tartrate solution was added to the sample. When the samples were cool, absorbance at 575 nm was measured with a spectrophotometer. The glucose concentration was determined by comparing absorbance with a standard curve.

## 4.6 Research approach

A summary of the experiments conducted is given in Table 4.3

Table 4.3: Research approach

Experiments conducted	Purpose of experiment
Determination of $k_{La}$ at different agitation rates and air flow rates in aerated stirred tank reactor	<ul style="list-style-type: none"><li>• Characterisation of vessel and comparison with literature</li><li>• Basis for comparison with venturi aeration</li></ul>
Determination of mixing time at different liquid flow rates and outlet heights in the venturi-aerated reactor	Establish if there were any mixing limitations in the tank and to determine the effect of mixing time on $k_{La}$
Measuring of $k_{La}$ at varying liquid flow rates in the venturi-aerated reactor	Determination of the effect of liquid flow rate in the venturi aerated reactor
Measuring of $k_{La}$ at varying venturi outlet height in the venturi-aerated reactor	Investigate any impact of bulk fluid movement in the tank on the $k_{La}$
Cultivation of <i>S. cerevisiae</i> in stirred tank reactor and venturi aerated reactor	Comparison of growth of cells in venturi system to that in stirred tank to establish any negative effect of the venturi aerator on the growth of yeast cells
Cultivation of <i>S. cerevisiae</i> in shake flasks with inoculum from venturi aerated reactor	Investigate viability of cells that have been through the venturi aerator

## 5 Results and discussion

### 5.1 Oxygen Mass Transfer in the Stirred Tank System

#### 5.1.1 OTR and $k_{La}$ as a function of agitation rate and gas flow rate

The change in DO concentration with time in the stirred tank was measured at different agitation and aeration rates. The explanation of the analysis of data for the calculation of  $k_{La}$  is given in Sections 4.2.3 and 4.2.4. The power supplied to the reactor for agitation was calculated from correlations given by Sinnott (2005:473) as described in Section 4.4.

The effect of agitation power and aeration rate on  $k_{La}$  in the stirred tank reactor are shown in Figure 5.1, across the operating ranges of aeration at 0 to 1.5 vvm and agitation power up to 7000 W m<sup>-3</sup>. The presence of air bubbles in the tank caused the agitation rate to vary because of the density change of the liquid –gas in the presence of an increasing fraction of air bubbles; this variation was less than 5%, i.e.:

$$\frac{\sqrt{(n_{gassed} - n_{ungassed})^2}}{n_{ungassed}} < 0.05$$

Surface aeration ( $k_{La}$  values up to 25% of maximum obtained at the same agitation rate), increased with agitation rate because of significantly greater surface disturbance. As expected,  $k_{La}$  increased with agitation rate. The error bars show standard deviation about the mean.

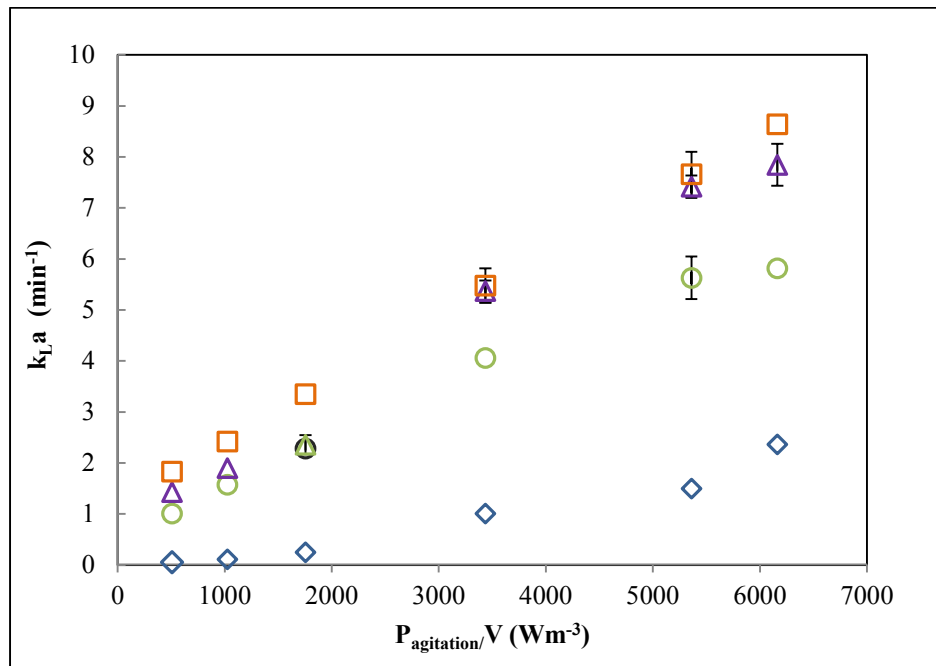


Figure 5.1: Variation of  $k_La$  with agitation rate at different air flow rates (0 L/min  $\diamond$ ; 12 L/min (0.7 vvm)  $\circ$ ; 16.5 L/min (1 vvm)  $\triangle$ ; 25 L/min (1.5 vvm)  $\square$ ). Error bars show standard deviation of three repeats.

Provision of air at 0.7 vvm resulted in a large increase in  $k_La$  relative to the un-aerated tank; however, improvement in  $k_La$  was small on further increasing the air flow rate. Doubling air flow rate from 0.7 vvm to 1.5 vvm resulted in an increase in  $k_La$  of about 1.5 times for the agitation between 1000  $\text{Wm}^{-3}$  and 6200  $\text{Wm}^{-3}$ , and 1.8 times at agitation at 509  $\text{Wm}^{-3}$ . This confirms the literature findings that at the lower agitation rate, increased air flow resulted in increased mass transfer area, while the effect is dampened at high agitation rates where  $k_La$  approaches a maximum (Gourich et al., 2008; Clarke et al., 2006; Atkinson & Mavituna, 1983). The low effect of aeration on  $k_La$  also implies that the air flow rates are high enough to neglect any changes in the oxygen concentration in the gas phase.

When  $k_La$  is correlated with Equation (2.23), the coefficients obtained, shown in Table 5.1, agree with those reported in literature, referenced in Table 2.2. This correlation fits the results obtained qualitatively, as can be seen from the solid lines in Figure 5.2. To obtain the  $k_La$  value excluding surface aeration, the value of  $k_La$  from surface aeration at that agitation rate was subtracted from the value of  $k_La$  for an aerated system. The resulting  $k_La$  was then correlated to power input and air velocity. In both cases, the coefficients obtained agreed with what is reported in literature.

Table 5.1: Coefficients for the correlation  $k_La = C \left(\frac{P}{V}\right)^\alpha u^\beta$

	Including surface aeration	Excluding surface aeration
$\alpha$	0.629	0.614
$\beta$	0.462	0.557
C	0.0058	0.008

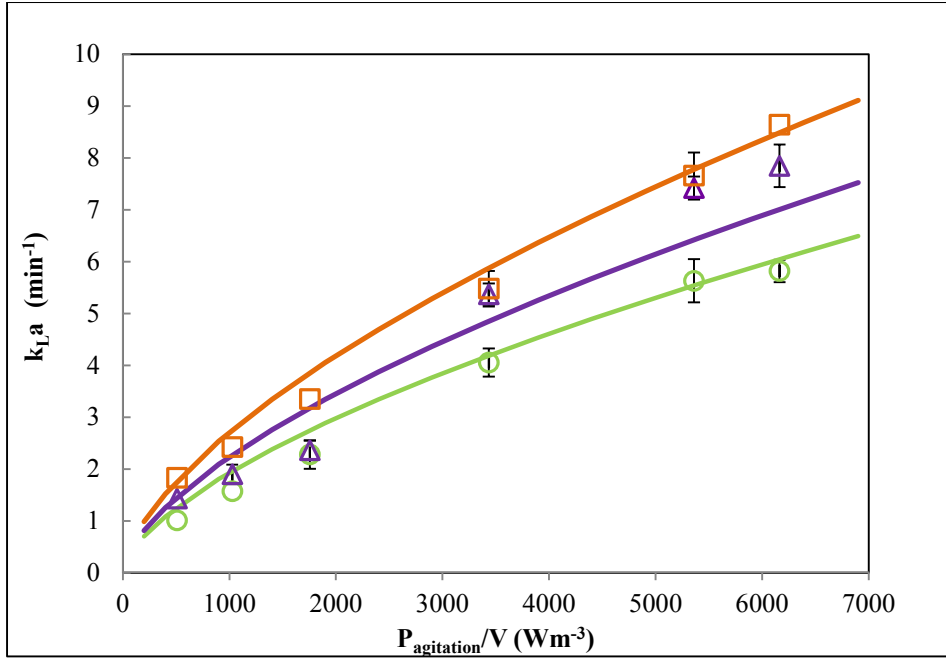


Figure 5.2: Solid lines show the correlation of  $k_La$  with aeration rate and agitation power input according to  $k_La = C \left(\frac{P}{V}\right)^\alpha u^\beta$  at different air flow rates (12 L/min  $\circ$ ; 16.5 L/min  $\triangle$  and 25 L/min  $\square$ )  $k_La$  values include surface aeration

The maximum calculated contribution of power input by the expanding gas in the reactor (Equation (2.31)) was found to be 12 % of the total agitation power. This was at an agitation rate of 509 W m<sup>-3</sup> and aeration of 25 L min<sup>-1</sup>. The correlation of  $k_La$  with  $P_{agitation}$  calculated this was expected to therefore yield similar results to Figure 5.2.

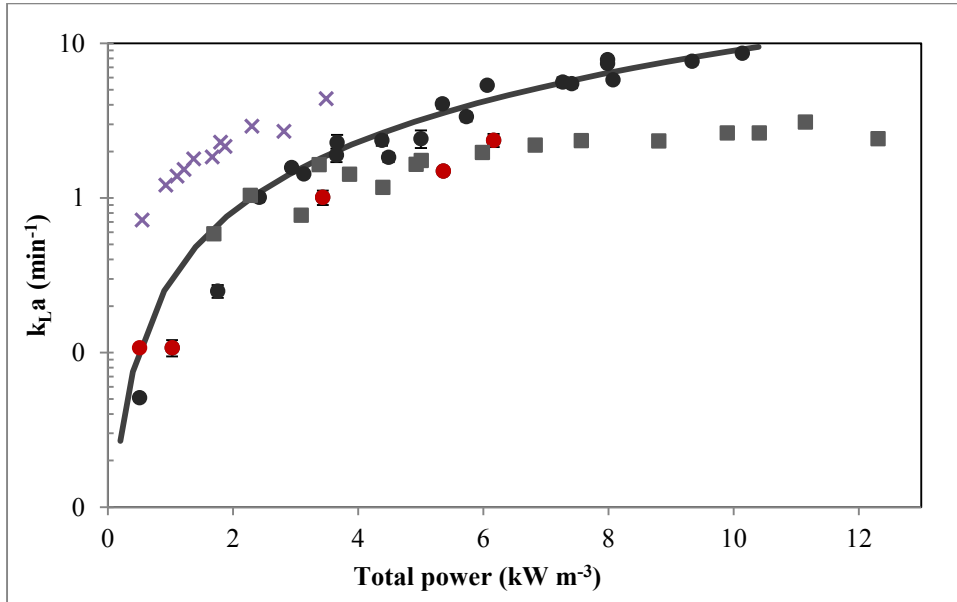


Figure 5.3: Variation of  $k_La$  in a stirred tank with total power input ( $\bullet$  experimental values from this study at different aeration rates with error bars showing standard deviation about the mean from three repeats;  $\bullet$  experimental values at no aeration;  $\text{—}$   $k_La = 0.00488 (P/V)^{1.49}$  (Eqn 5.1);  $\times$  Chandrasekharan & Calderbank, 1981;  $\blacksquare$  Robinson & Wilke, 1973)



The correlation between  $k_La$  and total power is investigated in Figure 5.3, where total power is the combination of agitation and compression power input. Using the sum of least squares and Microsoft Excel Solver, experimental  $k_La$  data from this study was fitted to give Equation (5.1):

$$k_La = 0.00488 \left( \frac{P_{total}}{V} \right)^{1.49} \quad (5.1)$$

The values used in the correlation includes mass transfer from both sparging and surface aeration, but  $k_La$  values from surface aeration only were omitted from the analysis because they showed an offset from the trend displayed by the rest of the experiments.

Based on air flow rates and agitation power consumption reported, the total power input in studies by Chandrasekharan & Calderbank (1981) and Robinson & Wilke (1973) was calculated and compared to the results from this study, also shown in Figure 5.3. Chandrasekharan & Calderbank (1981) operated at air flow rates between 0.16 vvm and 1 vvm in a 1.43 m<sup>3</sup> tank, while Robinson & Wilke (1973) used aeration rates between 0.5 and 1.5 vvm in a 2.5 L tank, both using the Rushton turbine and standard geometry in water. As with comparisons in agitation power input, the form of the equation holds but the equation constants differ for the different studies as shown in Table 2.2, further illustrating the variation of  $k_La$  even with similar operating conditions.

## 5.2 Oxygen mass transfer in the venturi system

When liquid flows through the venturi throat, air is drawn into the liquid stream and dispersed in the form of small bubbles (Cramers, 1992; Bauer, 1963). The liquid stream containing air bubbles then mixes with the rest of the fluid in the tank where the bubbles rise out of the liquid as the gas disengages from the liquid. Oxygen transfer into the liquid phase has been shown to happen in the outlet of the venturi (Rodriguez et al., 2012; Jackson, 1964) as well as in the tank (Gourich et al., 2007). Figure 5.4 prediction of variation of liquid pressure drop across the venturi throat and air flow rate into the venturi with liquid flow rate as predicted by Equations (2.24) and (2.25) respectively which are explained in Section (2.5). The  $k_La$  is expected to increase with liquid flow rate because more air is entrained into the liquid and also because more liquid is aerated with each pass through the venturi. The increased pressure drop is associated with high shear rates (Son, 2007) which could result in better bubble formation and improved mass transfer area.

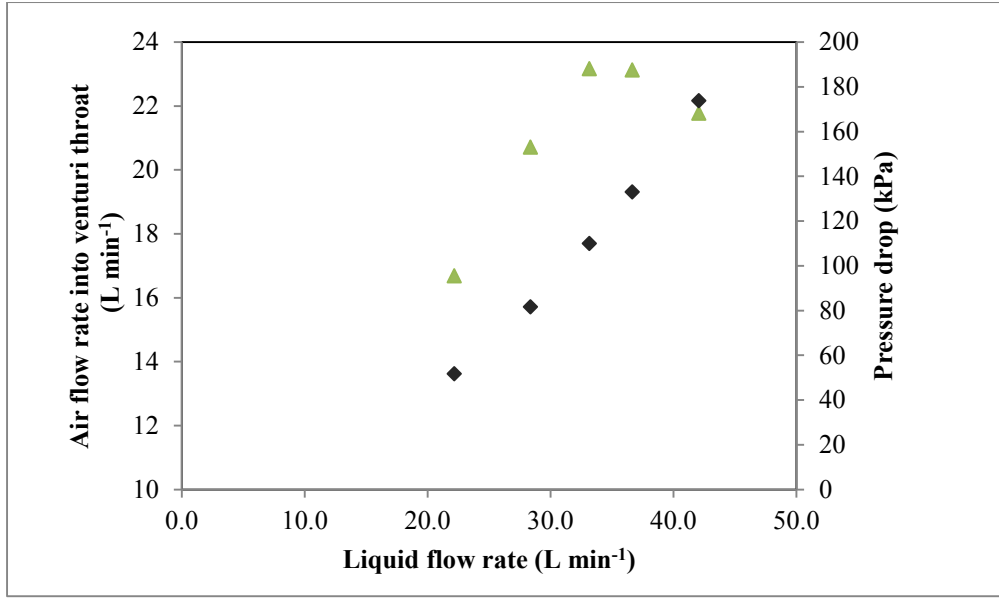


Figure 5.4: Prediction of the variation of liquid pressure drop in the throat of the venturi aerator (◆) and air flow rate into the venturi (▲) with liquid flow rate through the venturi

$$P + \frac{1}{2}\rho v^2 + \rho gh = \text{constant} \quad (2.24)$$

$$Q_G = CA \sqrt{2 g_c \rho \pi_1 \left( \frac{\gamma}{\gamma - 1} \right) \left[ \left( \frac{\pi_1}{\pi_2} \right)^{\frac{2}{\gamma}} - \left( \frac{\pi_1}{\pi_2} \right)^{\frac{\gamma+1}{\gamma}} \right]} \quad (2.25)$$

The change in DO concentration with time of deoxygenated water was measured 15 cm downstream of the venturi throat as the water was passed through the venturi. DO concentration was also measured in the tank. Further details of the experimental setup and procedure have been given in Section 4.1.2.

In Figure 5.5, dissolved oxygen concentration is presented as a function of time at both the outlet from the venturi loop and in the bulk fluid in the tank. These trends show that the water exiting the venturi became oxygen saturated more quickly than that in the tank, but did not become immediately saturated, as expected based on literature (Rodriguez, 2012). The liquid leaving the venturi is expected to be saturated with oxygen because there is good air flow rate and area for mass transfer to occur in the venturi and the outlet. The results thus imply that the aerator and outlet volume are too small to allow sufficient contact time for the liquid to be saturated with oxygen. The saturation concentration in the divergent outlet was the same as in the tank therefore it was assumed that the fluid at this point is at atmospheric pressure.

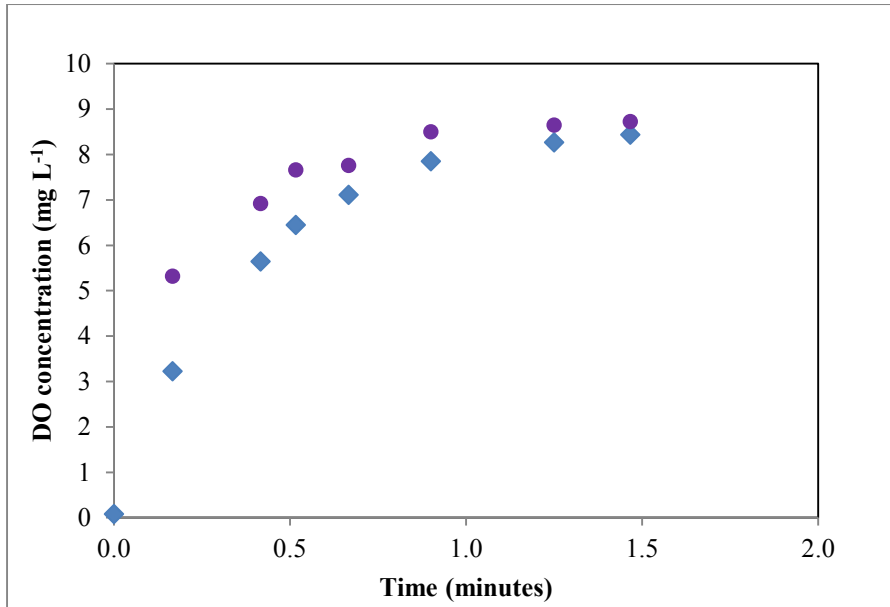


Figure 5.5: DO concentration in liquid stream immediately out of the venturi aerator (●) compared to DO concentration in the tank (◆) corrected for electrode response time at liquid flow rate of 36.6 L/min and 4 cm outlet height

The degree of surface aeration, determined by pumping liquid through the aerator with the air hole closed, was found to be minimal. Figure 5.6 shows how when the air hole is closed, DO concentration initially rises and then levels off without reaching saturation. The initial rise happens over about 10 minutes, almost ten times longer than it takes to reach DO saturation concentration when the air hole is open, as illustrated in Figure 5.5. The increase in DO concentration at the start may be attributed to a small amount of air that is accidentally drawn into the aerator and continually recycled until all the oxygen in the trapped gas bubbles has all dissolved into the water. Based on this, surface aeration was assumed to play a negligible role in oxygen mass transfer for the venturi-aerated reactor.

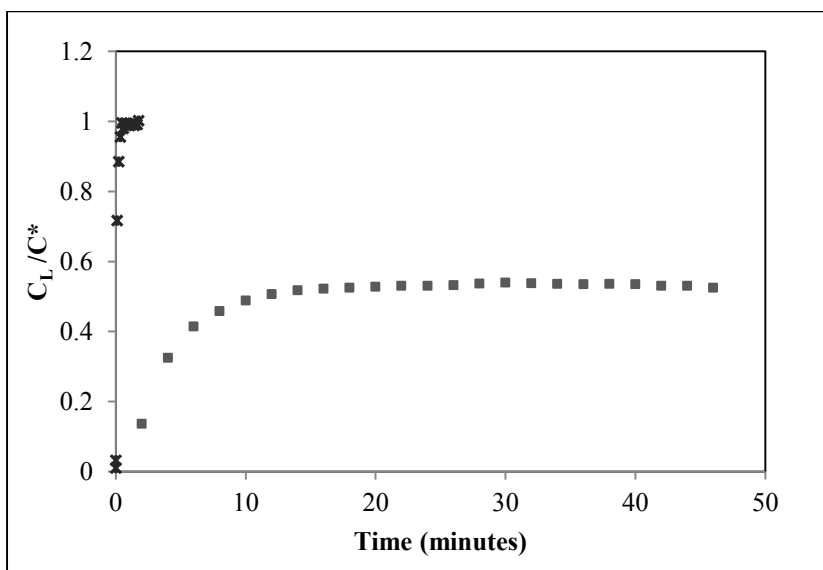


Figure 5.6: Change in DO concentration in the tank with time when the air hole is closed(■) compared to when the air hole is open (×). Liquid flow rate through the venturi aerator was 42 L min<sup>-1</sup> at a venturi outlet height of 8 cm

The  $k_{La}$  was calculated using Equation (2.11) and was found to be as much as ten times higher than in other venturi literature studies (Jackson, 1964; Gourich, 2007; Dong et al., 2011). Besides differences in reactor geometries and methods for determination of  $k_{La}$ , this difference could be a result of the much higher circulation of liquid through the venturi ( $\frac{Q_L}{V}$ ) (between 1.4 and 2.6 vvm in this study, compared to an average of 0.5 vvm in other studies). To address these postulations, the effects of liquid flow rate and venturi configuration are investigated in Sections 5.3.2 and 5.3.3 respectively.

### 5.2.1 Mixing in the tank

The mixing times for Setup 1, described in Section 4.1.2, at different outlet heights were investigated by measuring the change in conductivity in the solution. The results are shown in Figure 5.7. For the various operating conditions, steady state was established within 10 seconds (a quarter of the residence time of the tank), supporting the assumption that the agitation from the flow of water is enough to result in a well-mixed regime in the tank. These mixing studies do not provide an estimate for the residence time of gas bubbles, but give an indication of how quickly aerated water is distributed around the vessel.

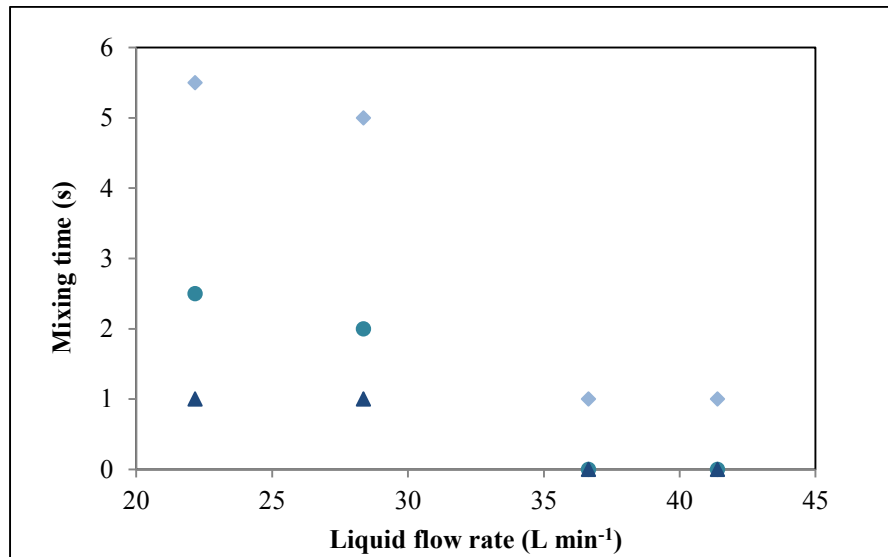


Figure 5.7: Mixing times in venturi aerated tank for a single venturi (Setup 1) at different venturi outlet heights from the bottom (4 cm ◆; 8 cm ● and 12 cm ▲) as a function of liquid flow rate. The values shown are average values with the standard deviation too small for the error bars to be visible.

As expected, the mixing time decreased with higher water flow rates for each height. Higher water flow rates imply that the water stream entering the tank has a higher velocity and greater momentum,

causing more bulk liquid movement and turbulence in the tank (Bauer, 1963). These are observed visually and lead to faster elimination of concentration gradients. Mixing time also decreased with increasing outlet height for the three outlet heights investigated. This may be attributed to differing flow regimes in the vessel for the different outlet heights.

Faster mixing times translate to quicker distribution of air bubbles which corresponds to higher observed  $k_La$ . If air bubbles are immediately spread around the tank,  $C^*$  is kept at the maximum value, while OTR is maximised. On the other hand, if there is slow circulation of fresh air bubbles,  $C^*$  in Equation (2.11) is overestimated, while the oxygen transfer rate is low. This would result in  $k_La$  calculated being lower than the actual  $k_La$ . Slow mixing is therefore expected to correspond to low apparent  $k_La$  values.

$$OTR = k_L a_T (C_L^* - C_L) \quad (2.11)$$

### 5.2.2 *OTR and $k_La$ as a function of liquid flow rate and depth of inlet (tank hydrodynamics)*

The  $k_La$  in a venturi-aerated system was evaluated using Equation (2.11) from DO concentration–time profiles illustrated in Figure 4.7. As explained in Section 4.2.5 this mass balance does not describe the venturi system accurately. However, the single value of  $k_La$  obtained using this method is representative of the average overall mass transfer and can be compared to the aerated stirred tank.

Figure 5.8 shows  $k_La$  obtained for Setup 1 at different venturi outlet heights and water flow rates. For each outlet height, higher flow rates resulted in higher  $k_La$ . In the range investigated,  $k_La$  continued to increase with flow rate and did not reach a critical flow rate where any further rise would have resulted in reduced  $k_La$  because of cavitation of the venturi or unfavourable flow regimes as in the studies of Briens et al. (1992) and Jackson (1964).

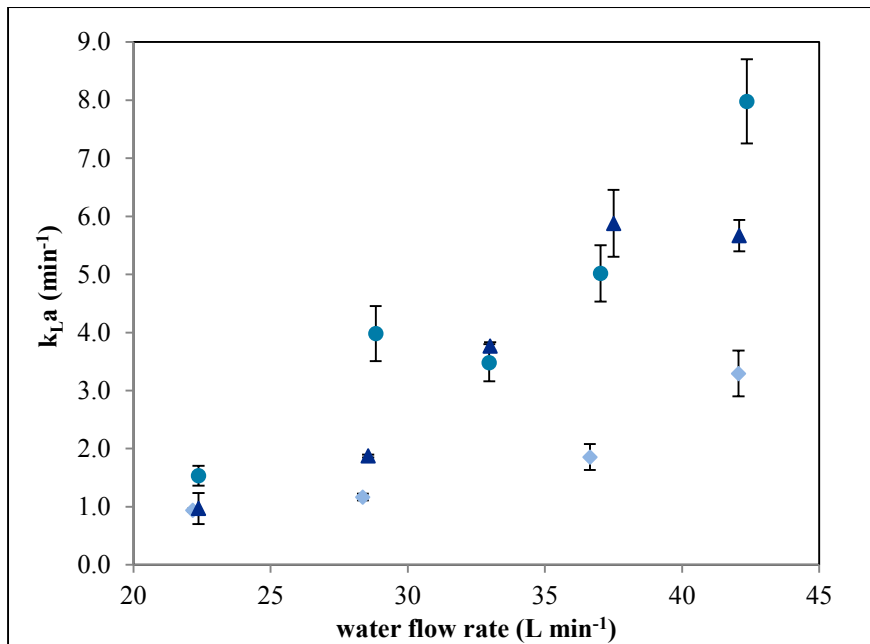


Figure 5.8: Effect of water flow rate and venturi outlet height from the bottom (4 cm ♦; 8 cm ●; 12 cm ▲) on  $k_La$ . Error bars show standard deviation from three repeats.

Higher flow rates of water gave greater air suction (

Table 5.2) as expected from Equations (2.24) and (2.25), with the predicted flow rates being slightly higher than those measured. The rate of air suction did not vary with outlet height. The ratio  $Q_G/Q_L$  was independent of outlet height and liquid flow rate in these ranges. As more water per unit time is exposed to air; higher  $k_La$  is expected. The increase in  $k_La$  with water flow rate may also be a result of the formation of smaller additional air bubbles, shown in Figure 5.9, resulting from higher turbulence and shear forces in the venturi as proposed by Bauer (1963). Furthermore, as discussed in the mixing results, improved distribution of air bubbles could also result in better oxygen mass transfer.

Table 5.2: Rate of air suction into the venturi for varying water flow rates. The air suction rate was not affected by the venturi outlet height.

Water flow rate (L min <sup>-1</sup> )	Air flow rate (L min <sup>-1</sup> )	$Q_G/Q_L$
22.2	13	0.59
28.4	19	0.67
33.2	20	0.60
36.6	22	0.60
41.4	23	0.56

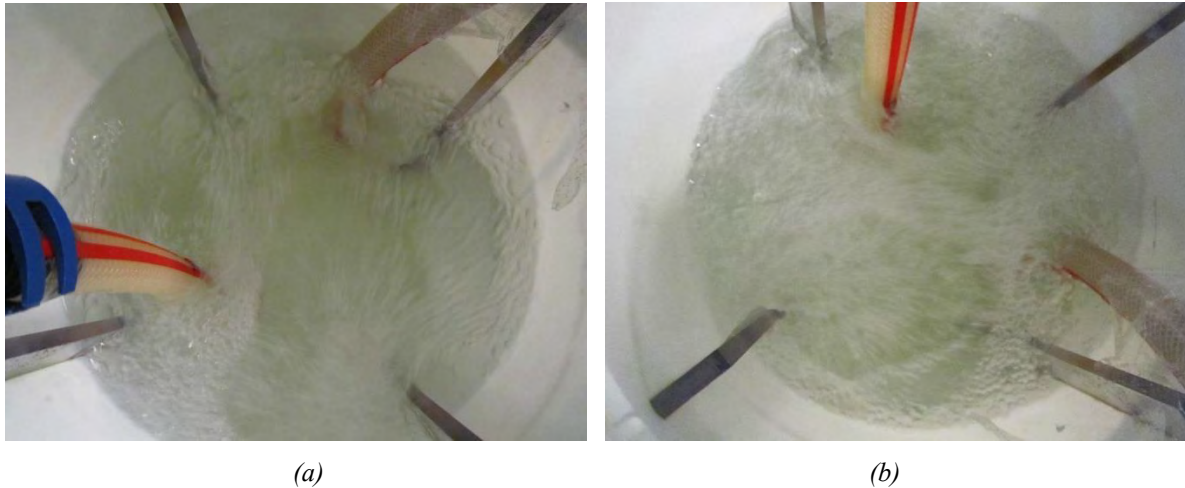


Figure 5.9: Comparison of gas holdup at (a) 22.2 L/min and (b) 36.6 L/min for a venturi outlet height of 12 cm

Increasing the venturi outlet height from 4 cm to 8 cm resulted in  $k_{La}$  values about 2.5 times higher, whereas a further increase from 8 cm to 12 cm made little difference. This agrees with the results obtained by Gourich et al. (2008) where the effect on  $k_{La}$  of changing the height of liquid in the tank was reduced with increasing flow rate at liquid heights of 1.12 m and 0.75 m. Gourich et al. (2008) also found that  $k_{La}$  was much lower when the liquid height was 0.37 m compared to greater heights. Their experiments were done at constant liquid volume.

As indicated in the mixing study, changing the outlet height had an effect on bulk movement of liquid in the vessel. A reason for the improvement in  $k_{La}$  could be that at 4 cm outlet height, there was short circuiting because of the proximity of the venturi outlet to the pump suction. A considerable fraction of the freshly aerated liquid could be sucked back into the pump immediately; thus reducing the residence time of bubbles in the tank, as well as minimising mixing of oxygen-rich water with oxygen-poor water. The corresponding improvement of  $k_{La}$  with reduced mixing time also suggests better distribution of air bubbles in the tank at the higher outlet heights due to the different flow patterns in the tank. The difference in  $k_{La}$  between 4 cm and the other outlet heights could mean that bulk liquid movement at 4 cm outlet height depressed mass transfer, supporting the suggestion of short-circuiting happening at this height. It could also imply that as long as the tank was perfectly mixed, bulk liquid movement did not have an effect on gas-liquid mass transfer.

Based on the mixing study,  $k_{La}$  is expected to vary more for different outlet heights at lower water flow rates. On the other hand Figure 5.8 shows  $k_{La}$  varying less with outlet height at flow rates of 22 L min<sup>-1</sup> and 28 L min<sup>-1</sup>. This means that at these flow rates,  $k_{La}$  cannot be improved by changing hydrodynamics in the tank, implying that the amount of air drawn into the aerator at low liquid flow rates is insufficient for good mass transfer to occur, even with favourable hydrodynamics in the vessel.

Variation in the lumped  $k_{La}$  term with tank hydrodynamics implies that oxygen mass transfer was not limited to the venturi aerator. Optimising fluid flow inside the tank had a considerable effect on the rate of mass transfer. The liquid flow rate through the venturi aerator should be high enough to entrain sufficient air and form sufficient bubbles. In addition, the bulk liquid movement in the tank should facilitate good mixing and long residence time of bubbles in the reactor.

### 5.2.3 *OTR and $k_{La}$ as a function of venturi configuration*

Two venturis were connected in parallel as described in Section 4.1.2 and the  $k_{La}$  was calculated from the change in DO concentration in the tank. Figure 5.10 shows the comparison of the  $k_{La}$  with liquid flow rate for the venturis in parallel to that for a single venturi (previously presented in Figure 5.8). The flow rate shown for the aerators in parallel is the total flow rate of the recirculated liquid, therefore the flow through individual aerators is less than when a single aerator was used. At the highest total flow rate of  $37 \text{ L min}^{-1}$ , the flow through either individual aerator is less than  $25 \text{ L min}^{-1}$ . The rate air drawn through each aerator roughly corresponds to that drawn in a single aerator at the same liquid flow rate ( $15 \text{ L min}^{-1}$ ), meaning the total amount of air supplied to the tank for two aerators in parallel was more than that supplied to the tank by a single aerator for the same total flow rate, although this higher air supply was not matched by improved  $k_{La}$  values for two venturis. This suggests that high liquid flow rates in the aerator are necessary for good mass transfer rates. A possible explanation for this is that high liquid flow rates in the venturi are associated with high shear rates that result in numerous small bubbles, causing improved mass transfer area and, subsequently, high  $k_{La}$ .



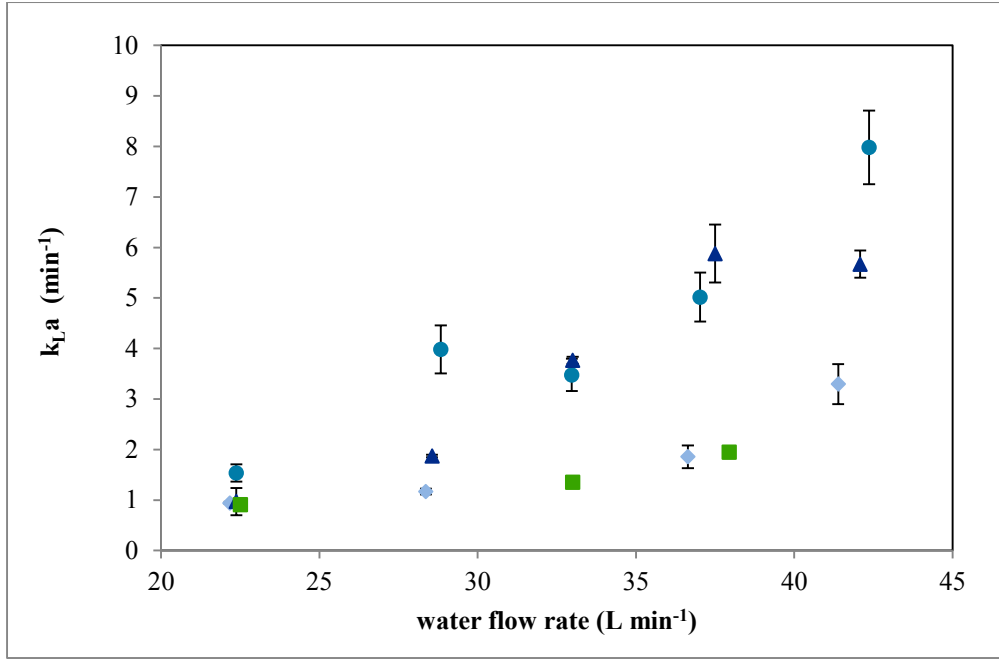


Figure 5.10: Comparison of  $k_L a$  between a single venturi at venturi outlet heights of 4 cm (♦), 8 cm (●) and 12 cm (▲), and two venturis connected in parallel at an outlet height of 8 cm (■). Error bars show standard deviation from the mean for three repeats.

#### 5.2.4 Modelling oxygen mass transfer using the Venturi system

The  $k_L a$  reported in Sections 5.2.2 and 5.2.3 gives overall performance of the venturi aeration system for the different operating conditions. However, to better understand oxygen mass transfer in the tank and aerator separately, mass balances on oxygen in the liquid phase were derived, shown in Equations (4.2) and (4.3) and their development given in Section 4.2.5.

To evaluate mass transfer coefficients in the venturi aerator ( $k_L A_V$ ) and the stirred tank ( $k_L a_T$ ) separately, theoretical  $C_V$  and  $C_L$  were fitted to the measured concentrations.

$$C_V = \frac{k_L A_V C_V^* + F C_L}{F + k_L A_V} \quad (5.2)$$

$$C_L = \left( C_{L,0} - \frac{\alpha}{\beta} \right) e^{-\beta t} + \frac{\alpha}{\beta} \quad (5.3)$$

where  $\alpha = \frac{F}{V_T} \left( \frac{k_L A_V C_V^*}{F + k_L A_V} \right) + k_L a_T C_L^*$  and  $\beta = k_L a_T - \frac{F}{V_T} \left( \frac{F}{F + k_L A_V} - 1 \right)$

If it is assumed that there is no mass transfer occurring in the tank, that liquid gets oxygenated only by passing through the venturi; then  $k_L a_T$  can be set to zero. Figure 5.11 shows that  $C_L$  predicted this way

is lower than actual  $C_L$  measured, confirming that mass transfer not only happens in the venturi outlet, but in the tank as well.

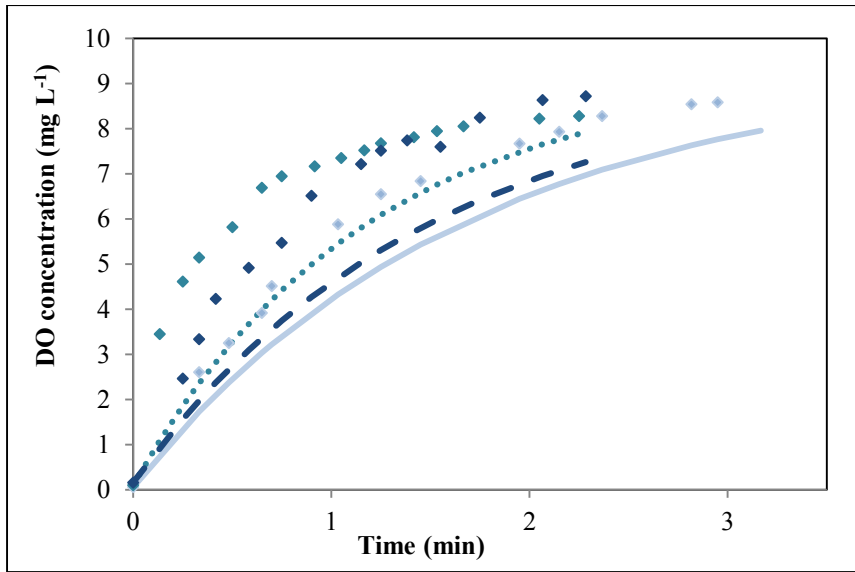


Figure 5.11: Difference between measured DO concentration at outlet heights of 4cm (♦), 8 cm (●) and 12 cm (▲), and that predicted by assuming no mass transfer happens in the tank at outlet heights of 4cm(—), 8 cm (···) and 12 cm (- - -).

Figure 5.12 shows  $k_L A_V$  and  $k_L a_T$  determined using Equations (5.2) and (5.3) and their variation with liquid flow rate and venturi outlet height.

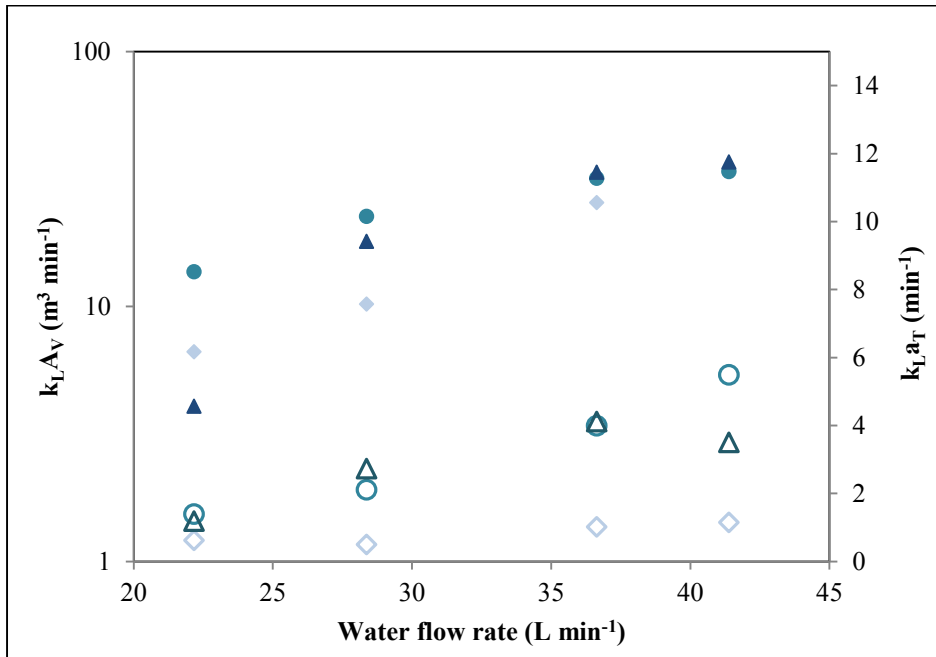


Figure 5.12: Effect of liquid flow rate and outlet height on  $k_L A_V$  at different venturi outlet heights (4 cm ♦ ; 8 cm ● and 12 cm ▲) and  $k_L a_T$  at different venturi outlet heights (4 cm ◇; 8 cm ○; 12 cm △). The models are based on averages of measured DO concentration with time.

At outlet heights 4 cm  $k_{LaT}$  is much lower than at outlet heights of 8 cm and 12 cm but at 22 L min<sup>-1</sup> the variation is smaller, confirming that the low  $k_{La}$  values at these low flow rates are a result of limitations in the venturi aerator and any improvements in  $k_{La}$  that would be due to better mixing in the tank are not realised. However, there is still mass transfer occurring in the tank even at these low liquid flow rates as shown by Figure 5.11.

At 8 cm and 12 cm,  $k_{LaT}$  increases with water flow rate possibly because more air is drawn to the reactor, therefore the number of bubbles formed increases and the flow patterns in the reactor are conducive for better mass transfer. At the outlet height of 4 cm,  $k_{LaT}$  stays constant at all liquid flow rates, indicating that improvements in  $k_{La}$  with liquid flow rate at 4 cm outlet height result only from an increase in  $k_{LaV}$  i.e. there is little contribution to mass transfer in the tank. Short circuiting at this height may also have prevented the distribution of aerated liquid from the venturi throughout the whole tank. In addition to the differing bulk liquid movement at the different outlet heights, the residence time of air bubbles in the tank could also have varied, as suggested by Briens et al. (1992) in their investigations of upflow and downflow venturi configurations. At 8 cm and 12 cm outlet heights, the residence time of the bubbles in the reactor may have been higher than at 4 cm due to the increased distance that the liquid exiting the venturi has to travel. Therefore, the gas holdup at these heights would be higher, resulting in increased surface area and, consequently, a higher  $k_{LaT}$ .

The mass transfer coefficient in the venturi ( $k_{LaV}$ ) increased with increasing water flow rate for all outlet heights, possibly as a result of better bubble formation in the venturi throat and outlet. At liquid flow rates of 22 L min<sup>-1</sup> and 28 L min<sup>-1</sup>  $k_{LaV}$  unexpectedly changed with outlet height. It was not established why mass transfer characteristics in the venturi aerator would vary with outlet height, which only affects bulk liquid movement inside the tank.

The results show that high liquid circulation rates correspond to better  $k_{La}$ , and that at these high flow rates,  $k_{LaT}$  controls the overall mass transfer coefficient since  $k_{LaV}$  appears to reach a maximum.

### 5.2.5 *Comparison of power input between stirred tank and venturi aerated tank*

The total power input to the reactor systems at all operating conditions was compared and the results are shown in Figure 5.13. The power input to the venturi-aerated reactor was calculated from the power discharged by the pump using Equation (2.33) as described in Section 4.4. The specific power input ( $P/V$ ) was taken to be the power input per unit operating volume of the reactor.

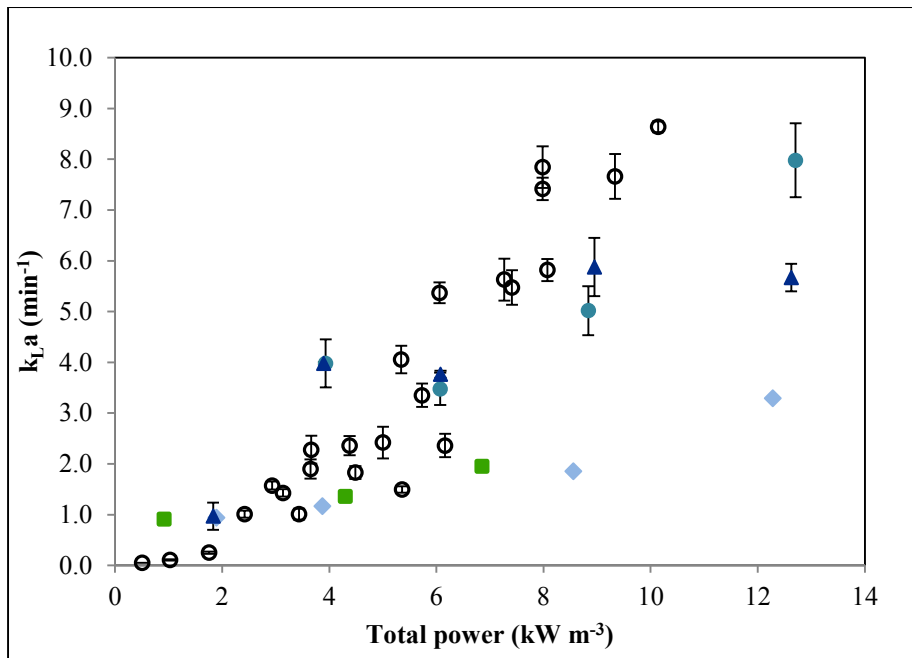


Figure 5.13: Variation of  $k_{La}$  with total power input for all conditions in the stirred tank reactor (○), Single venturi at outlet heights of 4 cm (◆); 8cm (●); 12 cm (▲) and two venturis in parallel at outlet height of 8cm (■). The error bars show standard deviation from the mean for three repeats.

At power input lower than  $6 \text{ kW m}^{-3}$ , the venturi aerated reactor and the stirred tank had similar  $k_{La}$ . At higher power input, variation of  $k_{La}$  in the venturi aerator with power input depended on the setup of the reactor, while  $k_{La}$  continued to increase in the stirred tank.

The calculation of power depends very much on the system and assumptions made. Calculations for energy input to compress gas assumed 100% efficiency and that air was compressed to 2 bar from atmospheric pressure, therefore changing the outlet pressure in the calculations would result in different results. For instance, if the air was compressed to 3 bar, the aerated stirred tank would show higher power input for the same  $k_{La}$ .

### 5.3 Yeast growth and survival in the Venturi aerated system

*S. cerevisiae* was cultivated in the aerated stirred tank, in the venturi -aerated reactor and in shake flask under non-sterile conditions as described in Section 4.5. The shake flasks were inoculated with cells that had been through the venturi for different periods. A summary of the growth characteristics is given in Table 5.3. The maximum growth rate of cells in a venturi-aerated system appeared higher at lower glucose consumption rate compared to the aerated stirred tank. However, more experiments would need to be conducted at different conditions in both reactors in order to establish whether there is a trend in the growth of yeast in the two reactor systems.

From Figure 5.14 the growth of brewer's yeast in a venturi aerated reactor was similar to that in a stirred tank. Under the conditions investigated, shear rates in the venturi aerator were not high enough to damage yeast cells. Figure 5.15 shows that cells that had been through the venturi aerator remained viable in shake flasks.

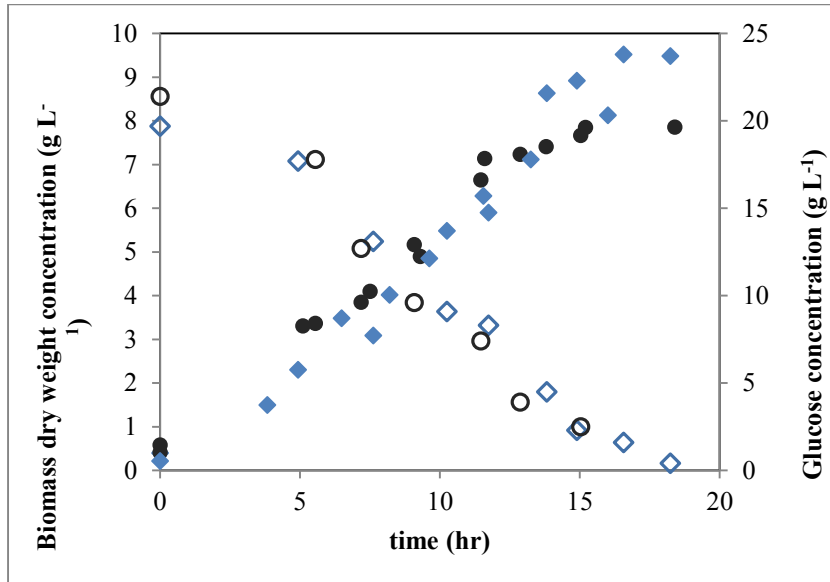


Figure 5.14: Comparison of growth of *S. cerevisiae* in the venturi aerated reactor (♦) to that in the stirred tank (●), and glucose consumption in the venturi aerated reactor (◇) and in the stirred tank (○). The growth data shown is for two repeats

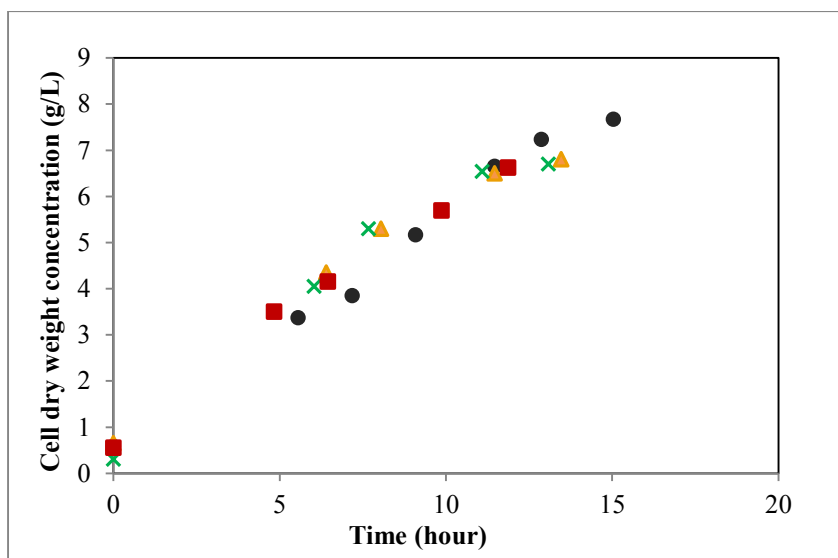


Figure 5.15: Growth of *S. cerevisiae* shake flask inoculated with cells from the aerated stirred tank (×) and cells that had been in the venturi aerated reactor for 15 minutes (▲) and 90 minutes (■) compared to growth of *S. cerevisiae* in the aerated stirred tank (●). The results shown are the mean of two repeats.

Table 5.3: Results for the cultivation of yeast in different reactor setups

	Maximum growth rate (h <sup>-1</sup> )	Maximum cell dry weight concentration after 15 hours (g L <sup>-1</sup> )	Glucose utilisation at maximum growth rate (g L <sup>-1</sup> h <sup>-1</sup> )
Aerated stirred tank	0.115	7.67	1.75
Venturi-aerated reactor	0.138	8.81	1.44
Shake flasks (average)	0.109	6.98	1.41

## 6 Conclusions and Recommendations

### 6.1 Conclusions

A comparison in  $k_{La}$  and energy input between an aerated stirred tank and a venturi-aerated reactor was conducted. This was done in order to determine whether the energy-intensive compression of air could be avoided in aerobic bioprocesses in order to reduce operating cost and environmental impact of bioreactors. The growth of yeast cells in a venturi aerated reactor was compared to that in an aerated stirred tank to establish whether the cells could survive shear stresses created in the venturi aerator.

Increasing volumetric liquid flow rate through the venturi resulted in improved  $k_{La}$  and oxygen mass transfer rates as more water is aerated per unit time, and possibly higher shear rates that resulted in more bubbles, giving greater surface area for mass transfer to occur. Higher liquid flow rates into the tank may additionally have resulted in faster mixing and distribution of air bubbles in the tank, also resulting in improved mass transfer.

Changing the outlet height of the venturi from 4 cm to 8 cm affected bulk liquid movement in the tank, as evidenced by the differing mixing times at different outlet heights for the same flow rates. At the higher liquid flow rates, faster mixing time corresponded to higher  $k_{La}$  values, suggesting that hydrodynamic conditions in the vessel affect the rate of mass transfer. On the other hand, at low flow rates, the improved mixing time with increased outlet height did not correspond to improved  $k_{La}$ , supporting the inference that high liquid flow rates result in high mass transfer area, and any improvements in bulk fluid flow in the tank would be insufficient to facilitate for mass transfer if not matched by a supply of fresh air bubbles to the tank. The venturi outlet height may also have affected the bubble residence time in the tank, with improved  $k_{La}$  at higher outlet heights.

The  $k_{La}$  achieved in the venturi aerated reactor was comparable to that of the stirred tank when the total power input was low. However, at higher power input to the reactors, corresponding to higher volumetric liquid flow rate in the venturi system, oxygen mass transfer rates are better in the aerated stirred tank.

There were no significant observed difference between the viability of brewer's yeast grown in the aerated stirred tank and that grown in the venturi-aerated reactor.

These findings are specific to the system used in this study, but they provide insights into the performance of venturi aerators.

## 6.2 Recommendations

In order to obtain high mass transfer rates, venturi aerated reactors should be operated at high liquid flow rates. If liquid flow rates are high enough and bulk liquid movement in the tank is not limited, then the optimisation of energy input vs mass transfer should be focused on minimising pressure losses associated with pumping the liquid through the venturi. Venturi aerator performance could be enhanced by reducing friction losses in the piping and therefore achieving higher liquid flow rates at lower power input to the pump.

Gourich et al. (2008) report that changing from upflow configuration to downflow configuration increased residence time of bubbles in the tank, resulting in higher  $k_La$ . Therefore further investigations into improving operation of venturi aeration could focus on whether the residence time of air bubbles in the tank with downflow can be further increased to improve gas mass transfer rates.

In this study venturi aeration was found to be comparable to that in an aerated stirred tank. Energy consumption will however be dependent on the system being used, line losses in a venturi, and pressure and flow rate of air in a stirred tank.

This study did not establish venturi aeration to be considerably more energy efficient than an aerated stirred tank for the conditions investigated. It is however worth noting that a liquid pump will have less capital and maintenance costs than a gas compressor. Venturi aerators could also be used to aerate recirculated streams in some continuous reactor setups. Instead of using energy to sparge air into the reactor as well as pump recycled broth, the recirculated stream could be passed through a venturi aerator.

Further investigations with other microorganisms and in sterile conditions should be conducted in order to expand on the applicability of venturi aerators to biological systems.



## 7 Bibliography

- Atkinson, B. & Mavituna, F. 1983. *Biochemical Engineering and Biotechnology Handbook*. Surrey, United Kingdom: Macmillan Publishers Ltd.
- Bandaiphet, C. & Prasertsan, P. 2006. Effect of aeration and agitation rates and scale-up on oxygen transfer coefficient,  $k_{La}$  in exopolysaccharide production from *Enterobacter cloacae* WD7. *Carbohydrate Polymers*. 66 (2006): 216-228.
- Batterham, R.J., Hoffmann, W. A. & Conochie, D. S. 1994. A reactor. International patent B01F3/04, 5/04.
- Bauer, W.G., Fredrickson, A. G. & Tsuchiya, H. M. 1963. Mass transfer characteristics of a venturi liquid-gas contactor. *I & EC Process Design and Development*. 2 (3):178-187.
- Baylar, A., Ozkan, F. & Ozturk, M. 2006. Influence of venturi cone angles on jet aeration systems. *Water Management*. 58 (2005):9-16.
- Baylar, A. & Ozkan, F. 2006. Applications of venturi principle to water aeration systems. *Environmental Fluid Mechanics*. 6 (4): 341-357.
- Baylar, A., Unsal, M. & Ozkan, F., 2007. Determination of the optimal location of the air hole in venturi aerators. *CLEAN – Soil, Air, Water*. 35 (3): 246-249
- Bouaifi, M., Hebrard, G., Bastoul, D. & Roustan, M. 2001. A comparative study of gas hold-up, bubble size, interfacial area and mass transfer coefficients in stirred gas- liquid reactors and bubble columns. *Chemical engineering and processing*. 40 (2001): 97 – 111.
- Boyce, M. P. Transport and storage of fluids. 1999. In *Perry's Chemical Engineers' Handbook* 7<sup>th</sup> Edition. R. H. Perry & D. W Green, Eds. New York: McGraw-Hill. 10-37.
- Brar, S.K., Verma, M., Tyagi, R. D., Surampalli, R. Y., Barnabe, S. & Valero, J. R. 2007. *Bacillus thuringiensis* proteases: Production and role in growth, sporulation and synergism. *Process Biochemistry*. 42 (5): 773-790.
- Briens, C. L., Huynh, L. X., Large, J. F., Catros, A., Bernard, J. R. & Bergougnou, M. A. 1992. Hydrodynamics and gas-liquid mass transfer in a downward venturi-bubble column combination. *Chemical Engineering Science*. 47 (13): 3549-3556.
- Chandrasekharan, K. & Calderbank, P. H. 1981. Further observations on the scale up of aerated mixing vessels. *Chemical Engineering Science*. 36 (1981): 819-823.
- Chisti, Y. 2000. Animal-cell damage in sparged bioreactors. *TIBTECH*. 18 (2000): 420-432.

Chisti, M. Y. 1989. *Airlift Bioreactors*. London: Elsevier.

Chisti, M. Y. & Jauregui-Haza, U. J. 2002. Oxygen transfer and mixing in mechanically agitated airlift bioreactors. *Biochemical Engineering Journal*. 10 (2002): 143-153.

Clarke K.G., Williams P.C., Smit M. and Harrison S.T.L. (2006). Enhancement and repression of volumetric oxygen transfer coefficient through hydrocarbon addition and its influence on oxygen transfer rate in stirred tank bioreactors. *Biochemical Engineering Journal*. 28 (2006): 237-242

Correia, L.D. & Clarke, K.G., 2009. Measurement of the overall volumetric oxygen transfer coefficient in alkane-aqueous dispersions. *Journal of Chemical Technology & Biotechnology*. 84 (12): 1793-1797.

d'Hugues, P., Cezac, P., Cabral, T., Battaglia, F., Truong-Meyer, X. M. & Morin, D. 1997. Bioleaching of a cobaltiferous pyrite: a continuous laboratory-scale study at high solids concentration. *Mineral Engineering*. 10 (5): 507-527.

Deckwer, W. D., Burckhart, R., Zoll, G. 1974. Mixing and mass transfer in bubble columns. *Chemical Engineering Science*. 29 (1974): 2177-2188.

Dhanasekharan, K. M., Sanyal, J., Jain, A. & Haidari, A. 2005: A generalised approach to model oxygen transfer in bioreactors using population balances and computational fluid dynamics. *Chemical Engineering Science*. 60 (2005): 213-218.

Dong, C., Zhu, J., Wu, X. & Miller, C. F. 2012. Aeration efficiency influenced by venturi aerator arrangement, liquid flow rate and depth of diffusing pipes. *Environmental Technology*. 33 (11): 1-10.

Fakeeha, A. H., Jibril, B. Y., Ibrahim, G. & Abasaheed, A. E. 1999. Medium effects on oxygen mass transfer in a plunging jet loop reactor with a downcomer. *Chemical Engineering and Processing*. 38 (1999): 259-265.

Federal Emergency Management Agency. 1989. *Handbook of Chemical Hazard Analysis Procedure*. USA: Department of Transportation, and Environmental Protection Agency.

Galaction A. -I., Cascaval, D., Oniscu, C. & Turnea, M. 2004. Prediction of oxygen mass transfer coefficients in stirred bioreactors for bacteria, yeasts and fungus broths. *Biochemical Engineering Journal*. 20 (1): 85-94.

Gamisans, X., Sarrà, M. & Javier Lafuente, F. 2004. Fluid flow and pumping efficiency in an ejector-venturi scrubber. *Chemical engineering and processing*. 43 (2004): 127-136.

- Garcia-Ochoa, F. & Gomez, E. 2009. Bioreactor scale-up and oxygen transfer rate in microbial processes: An overview. *Biotechnology Advances*. 27 (2): 153-76.
- Gauthier, L., Thibault, J. & LeDuy, A. 1990. Measuring  $k_{La}$  with randomly pulsed dynamic method. *Biotechnology and Bioengineering*. 37 (1991): 889- 893.
- Germain, E., Nelles, F., Drews, A., Pearce, P., Kraume, M., Reid, E., Judd, S. J., Stephenson, T., 2007. Biomass effects on oxygen transfer in membrane bioreactors. *Water Research*. 41 (5): 1038-1044.
- Gibson, C. E. 1975. A field and laboratory study of oxygen uptake by planktonic blue-green algae. *Journal of Ecology*. 63 (3): 867-879.
- Gogate, P.R. & Pandit, A.B. 1999. Survey of measurement techniques for gas-liquid mass transfer coefficient in bioreactors. *Biochemical Engineering Journal*. 4 (1999): 7-15.
- Gogate, P.R., Beenackers, A. C. M. & Pandit, A.B. 2000. Multiple-impeller systems with a special emphasis on bioreactors: a review. *Biochemical Engineering Journal*. 6 (2000): 109-144.
- Gourich, B. N., Vial, Ch., Belhaj Soulami, M., Zoulalian, A. & Ziyad, M. 2008. Comparison of hydrodynamic and mass transfer performances of an emulsion loop-venturi reactor in co-current downflow and upflow configurations. *Chemical Engineering Journal*. 140 (2008): 439-447.
- Gourich, B., El Azher, A., Vial, Ch., Belhaj Soulami, M., Zoulalian A. & Ziyad, M. 2007. Influence of operating conditions and design parameters on hydrodynamics and mass transfer in an emulsion loop-venturi reactor. *Chemical Engineering and Processing: Process Intensification*. 46 (2): 139-149.
- Jackson, M. L. & Collins, W.D. 1964. Scale up of a venturi aerator. *I & EC Process Design and Development*. 3 (4): 386-393.
- Jackson, M. L., 1964. Aeration in Bernoulli types of devices. *AIChE Journal*. 10(6): 836-842.
- Joshi, J. B., Pandit, A. B. & Sharma, M. M. 1982. Mechanically agitated gas-liquid reactors: review article number 7. *Chemical Engineering Science*. 37 (6): 813- 844.
- Juteau, P., Tremblay, D., Ould-Moulaye, C., Bisailon, J-G. & Beaudet, R. 2004. Swine waste treatment by self-heating aerobic thermophilic bioreactors. *Water Research*. 38 (2004): 539-546.
- Kapic, A. & Heindel, T. J. 2006. Correlating gas-liquid mass transfer in a stirred tank reactor. *Chemical Engineering Research and Design*. 84 (A3): 239-245.

- Kargi, F. & Moo-Young, M. 1985. Transport phenomena in bioprocesses. In *Comprehensive Biotechnology: Volume 2*. M. Moo-Young, C. L. Clooney, A. E. Humphrey, Eds. Oxford: Pergamon Press.
- Kocabaş, P., Çalik, P. & Özdamar, T. H. 2006. Fermentation characteristics of L-tryptophan production by the acidophilic bacillus acidocaldarius in a defined medium. *Enzyme and Microbial Technology*. 39 (2006): 1077-1088.
- Liley, P. E., Thomson, G. H., Friend, D. G., Daubert, T. E. & Buck, E. 1999. Physical and chemical data. In *Perry's Chemical Engineers' Handbook* 7<sup>th</sup> ed. R. H. Perry & D. W Green, Eds. New York: McGraw-Hill. 2-127.
- Langheinrich, C., Nienow, A. W., Eddleston, T., Stevenson, N. C., Emery, A. N., Clayton, T. M. & Slater, N. K. H. 2002. Oxygen transfer in stirred bioreactors under animal cell culture conditions. *Trans IChemE*. 80 (March): 3-8.
- Linek, V., Benes, P., Sinkule, J. & Moucha, T. 1993. Non-ideal pressure step method for  $k_{La}$  measurement. *Chemical Engineering Science*. 48 (9): 1593- 1599.
- Linek, V., Vacek, V. & Benes, P. 1985. A critical review and experimental verification of the correct use of the dynamic method for the determination of oxygen transfer in aerated agitated vessels to water, electrolyte solutions and viscous fluids. *The Chemical Engineering Journal*. 34 (1987): 11-34.
- Linek, V. & Vacek, V. 1981. Chemical engineering use of catalyzed sulphite oxidation kinetics for the determination of mass transfer characteristics of gas-liquid contactors. *Chemical Engineering Science*. 36 (11): 1747-1768.
- McCabe, W. L., Smith, J. C., Harriot, P. 2011. *Unit Operations of Chemical Engineering* 6<sup>th</sup> ed. New York: McGraw- Hill.
- Merchuk, J. C. 1983. Basic models for mass transfer. In *Heat and Mass Transfer*. (AIChE Modular instruction series B: Stagewise and mass transfer operations). New York: AIChE.
- Mohaibes, M. & Heinonen-Tanski, H., 2004. Aerobic thermophilic treatment of farm slurry and food wastes. *Bioresource technology*. 95 (2004): 245-254.
- Muller, F. L. & Davidson, J. F, 1992. On the contribution of small bubbles to mass transfer in bubble columns containing highly viscous liquids. *Chemical Engineering Science*. 47 (13/14): 3525-3532.
- Nocentini, M., Fajner, D., Pasquali, G. & Magelli, F. 1993. Gas- liquid mass transfer and holdup in vessels stirred with multiple Rushton turbines: Water and water- glycerol solutions. *Industrial & Engineering Chemistry Research*. 32 (1): 19- 26.

Noorman, H. 2006. Mass transfer. In *Basic Biotechnology*. C. Ratledge & B. Kristiansen, Eds. New York: Cambridge University Press. 201 -217.

Obeta Ugwuanyi, J., 2008. Yield and protein quality of thermophilic *Bacillus* spp biomass related to thermophilic aerobic digestion of agricultural wastes for animal feed supplementation. *Bioresource Technology*. 99 (2008): 3279-3290.

Pandit, A.B., Niranjana, K. & Davidson, J. F. 1990. Pump-stirred aerator. *Chemical Engineering Science*. 46 (9): 2293-2301.

Puskeiler, R. & Weuster-Botz, D. 2005. Combined sulphite method for the measurement of the oxygen transfer coefficient  $k_{La}$  in bioreactors. *Journal of Biotechnology*. 120 (2005): 430-438.

Robinson, C. W. & Wilke, C. R. 1973. Oxygen absorption in stirred tanks: A correlation for ionic strength effects. *Biotechnology and Bioengineering*. 15 (1973): 755- 782.

Rodriguez, G., Dorado, A. D., Bonsfills, A., Sanahuja, R., Gabriel. D. & Gamisans, X. 2012. Optimization of oxygen transfer through venturi-based systems applied to the biological sweetening of biogas. *Journal of Chemical Technology & Biotechnology*. 87 (6): 854-860.

Rossi, G. 2001. The design of bioreactors. *Hydrometallurgy*. 59 (2-3): 217-231.

Ruchti, G., Dunn, I. J. & Bourne, J. R., 1981. Comparison of dynamic oxygen electrode methods for the measurement of  $k_{La}$ . *Biotechnology and Bioengineering*. 23 (1981): 277-290.

Sánchez Pérez, J. A., Rodriguez Porcel, E. M., Casas Lopez, J. L., Fernandez Sevilla, J. M. & Chisti, Y. 2006. Shear rate in stirred tank and bubble columns bioreactors. *Chemical Engineering Journal*. 124 (2006): 1-5.

Schluter, V. & Deckwer, W.-D. 1992. Gas/ liquid mass transfer in stirred vessels. *Chemical Engineering Science*. 47 (9-11): 2357- 2362.

Shukla, V. B., Parasu Veera, U., Kulkarni, P. R. & Pandit, A. B., 2001. Scale-up of biotransformation process in a stirred tank reactor using dual impeller bioreactor. *Biochemical Engineering Journal*. 8 (2001): 19-29.

Sinnot, R. K. 2005. *Chemical Engineering Design*. (Coulson & Richardson's chemical engineering volume 6). Oxford: Elsevier.

Son, Y. 2006. Determination of shear viscosity and shear rate from pressure drop and flow rate relationship in a rectangular channel. *Polymer*. 48 (2): 632-637.

Stenberg, O. & Andersson, B. 1988. Gas- liquid mass transfer in agitated vessels – I. evaluation of the gas- liquid mass transfer coefficient from transient-response measurements. *Chemical Engineering Science*. 43 (3): 719-724.

Stieger, K. 1999. *Mass Transfer Studies in the Lysine Fermentation*. MSc dissertation, Department of Chemical Engineering, University of Cape Town.

Suresh, S., Srivastava, V. C., Mishra, I. M., 2009. Techniques for oxygen transfer measurement in bioreactors: a review. *Journal of Chemical Technology and Biotechnology*. 84 (2009): 1091-1103.

Thalasso, F., Naveau, H. & Nyns, E.-J. 1995. Design and performance of a bioreactor equipped with a venturi injector for high gas transfer rates. *The Chemical Engineering Journal*. 57 (1995): B1-B5.

Treybal, R. 1955. *Mass Transfer Operations*. New York: McGraw-Hill Book Company.

Tribe, L., A., Briens, C., L. & Margaritis, A. 1995. Determination of the volumetric mass transfer coefficient ( $k_{La}$ ) using the dynamic “gas out- gas in” method: analysis of errors caused by dissolved oxygen electrodes: Communication to the editor. *Biotechnology and Bioengineering*. 46 (1995): 388-392.

Tromans, D. 1998. Temperature and pressure dependent solubility of oxygen in water: A thermodynamic analysis. *Hydrometallurgy*. 48 (1998): 327- 342.

van Hille, R., Johnstone-Robertson, M., Huddy, R., Smart, M., van Wyk, N., Ngoma E.& Harrison S.T.L. 2014. *CHE 5054 Introduction to Microbiology Laboratory Manual 2014*. Centre for Bioprocess Engineering, University of Cape Town.

Van’t Riet, K. 1979. Review of measuring methods and results in nonviscous gas-liquid mass transfer in stirred vessels. *Industrial & Engineering Chemistry Process Design and Development*. 18 (3): 357-364.

Villadsen, J., Nielsen, J. & Lidén, G. 2011. *Bioreaction Engineering Principles* 3<sup>rd</sup> ed. New York: Springer.

Welty, J. R., Wicks, C. E., Wilson, R. E. & Rorrer, G. L. 2001. *Fundamentals of Momentum, Heat and Mass Transfer* 4<sup>th</sup> ed. New Jersey. John Wiley & Sons Inc.

Wesselingh, J. A. & Krishna, R. 2000. *Mass Transfer in Multicomponent Mixtures*. Delft, The Netherlands: Delft University Press.

Williams, P. C. 2005. *Biological Conversion of Alkanes to Dicarboxylic Acids*. MSc dissertation, Department of Chemical Engineering, University of Cape Town.

Yan, G., Hua, Z., Liu, D., Du, G., Chen, J. 2006. Influence of oxygen level on oxidative stress response of bacillus sp. F26 to menadione. *Process Biochemistry*. 41 (2006): 764-769.

Yang, S-T. 2007. Preface. In *Bioprocessing for Value-Added Products From Renewable Resources: New Technologies and Applications*. S-T. Yang, Ed. Netherlands: Elsevier.